POLITECNICO DI TORINO

FACOLTÀ DI INGEGNERIA

Bachelor in Biomedical Engineering

BACHELOR'S FINAL PROJECT

DIPARTIMENTO DI INGEGNERIA MECCANICA E AEREOSPAZIALE

DEVELOPMENT OF CHITOSAN BASED HYDROGELS AS BIO-INKS FOR RAPID PROTOTYPING TECHNOLOGIES

Supervisors
Prof. Chiono, Valeria
Ph. D. Tonda Turo, Chiara

Author
Flores García, Marina

Abstract

The ongoing demand of organs is growing significantly in the last years. There are a lot of people who need a transplant and they are in the waiting list because there are not enough donors to supply all the people.

For that reason, fields as Tissue Engineering are studying new ways to create or restore tissues and organs. Among them, 3D bioprinting is emerging more popular and it consists in creating 3D tissue constructs with bioink, the material used to print, and pre-designed structures previously designed with computer-aided design. Bioink is a combination of biomaterials and living cells.

This project focuses its attention in finding a thermo-sensitive hydrogel, stable liquid solutions at refrigerated temperature that turn into gel upon an increase of temperature. They are composed of chitosan and a polyol-phosphate salt and they must serve as a bioink. Then, with the possible candidates as bioinks, studies of rheology and printability are performed.

Three candidates are the best ones to be used as bioinks for their low gelation time, the time in which the solution/gel transition occurs, and their pH similar to the physiological one. Further studies, as degradation tests, allow the selection of two of them as the best candidates.

Rheology studies help to understand the flow behaviour of the solutions and the viscoelastic properties of the solutions by measuring the storage modulus, which represents the elastic behaviour of the material, and the loss modulus, which represents the viscous behaviour.

Then, an exhaustive study on printability gives the best combinations of parameters that affect the final printed structures that are printed with the two candidates as bioink. These parameters are the state of the ink, the diameter of the nozzle, the addition or no addition of PBS solution to the printbed and the temperatures at which the syringe and the printbed must be.

Good results on bioprintring are achieved proving that the two thermo-sensitive solutions composed of chitosan and a polyol-phosphate salt are good candidates as bioinks.

Acknowledgements

First of all, I am grateful to Politecnico di Torino, in special to professor Valeria Chiono, for bringing me this good and amazing opportunity of collaborating with the Dipartimento di Ingegneria Meccanica E Aerospaziale (DIMEAS) in this research.

My sincere thanks to professor Chiara Tonda Turo, who has guided me and helped every moment in this research, and from who I have learnt a lot from her expertise.

I am also grateful to student Rosanna Fusaro, who stayed with me the first two months of the research collaborating together. I am thankful to her for her patience and for routing this study.

I take this opportunity to express gratitude to all of the laboratory members for their help and support.

I am very thankful to my laboratory mate, Itziar Egurbide, with who I have worked in big part of this study and we have helped each other every moment.

And last but not least, I also thank my family for their encouragement and support.

Glossary

β-GP	β-Glycerophoshate Disodium Salt Pentahydrate
CS	Chitosan
CS 80/100	Chitosan with 80% deacetylation degree, 100 kDa molecular weight average
CS 95/100	Chitosan with 95% deacetylation degree, 100 kDa molecular weight average
DMEM	Dulbecco's Modified Eagle Medium
EWC	Equilibrium Water Content
FBS	Foetal Bovine Serum
G'	Storage Modulus
G''	Loss Modulus
G1-P	α-D-Glucose-1-Phosphate Disodium Tetrahydrate
GP	Glycerolphosphate
HCl	Hydrochloric Acid
M	Molar
PBS	Phosphate-buffered saline
PP	Polyol-phosphate
R	Ratio
SC	Stem Cells
TE	Tissue Engineering
WL	Weight Loss

Index

1. Preface

1.1. Origin of the study

Nowadays, Tissue Engineering is a field that is notably growing and more techniques to regenerate tissue appear. Between them, 3B bioprinting has emerged a revolutionary technology as they have received significant interest in consumer, industrial and academic sectors.

The idea of printing a functional construct is not far from the future and many institutions are involved in projects with the aim of finding new methods or improving the ones that exist to develop biological substitutes that restore, maintain, or improve tissue function or a whole organ.

At LADISPE, a laboratory that belongs to the Dipartimento di Ingegneria Meccanica E Aerospaziale (DIMEAS) from Politecnico di Torino, a project on the development of thermo-sensitive hydrogels based on chitosan and polyol-phosphate salt was carried on. The first idea was to find a proper hydrogel with good characteristics to be printed and to incorporate cells inside for a further tissue regeneration.

1.2. Motivation

In the seventh semester of my Bachelor in Biomedical Engineering I attended the subject of Tissue Engineering. I learnt a lot in this subject and I discovered a field that was very interesting and fascinating. While I was attending the subject I was also involved in a project about 3D printing focused on bone regeneration.

Both things, the subject and the project, made me realize that this was the field I liked the most in Biomedical Engineering. For that reason, when I had to choose a thematic for my final project I decided a project on Tissue Engineering and professors from Politecnico di Torino offered me a project on Tissue Engineering using 3D bioprinting.

1.3. Previous requirements

Before starting this project, some previous knowledge concerning Tissue Engineering and good laboratories skills were needed. The knowledge in the field was acquired in the subject of “Tissue Engineering” and the laboratories skills were acquired in different subjects from the Bachelor in Biomedical Engineering at Universitat Politècnica de Catalunya.

Basic knowledge about 3D printing was needed in order to understand the 3D printer and the software. Moreover, good level in Solidworks was needed to design patterns to be printed; this knowledge had been acquired in the subject of "Graphic Design" imparted in the Bachelor.

Among these previous requirements, it was necessary to understand a previous master thesis that was being developed in LADIPSE by a master student. This project was the starting point of the study, where the best combinations and concentrations of chitosan and polyol-phosphate salts were selected in order to achieve hydrogels with low gelation time and pH in the physiological range.

1.4. Objectives

The main objective of this project is to obtain a hydrogel based on chitosan and polyol-phosphate salt with good characteristics in order to be printed. This study can be divided in two parts:

- A first part that would be the continuation of the master thesis that was being carried on by a master student and it comprises the development of the proper hydrogel with low gelation time and pH similar to the physiological pH. In this part, different concentrations of chitosan and polyol-phosphate salt are selected in order to improve the characteristics of the hydrogel for its printability. Different tests are performed to ensure the best characteristics.
- Then, a second part that is more focused on the study of printability and rheological analysis of the chosen hydrogels. An exhaustive rheological analysis is done to study the flow behaviour of the hydrogels. Knowing the flow behaviour of the hydrogel permits a better comprehension on the printability of them, allowing the variation of some parameters to achieve good results on bioprinting. Then, an exhaustive study on the selection of the best combination of these parameters is done.

1.5. Areas covered

This project covers the development of different hydrogels based on chitosan and polyol-phosphate salt, as well as all the required tests to ensure the best characteristics of the hydrogel. These tests control the gelation time of the hydrogel, the pH and the degradation of the hydrogel in contact with physiological environment.

It also covers the study and comprehension of rheological properties of the hydrogel by a series of rheological tests.

Moreover, this project includes all the part related with bioprinting, its functioning, the design of different patterns to be printed with Solidworks and the study of different combination of parameters that ensure the best results on bioprinting.

2. Introduction

Despite everyday new advances in medicine and technology appear, and more people is aware of organ donation and transplantation, there is a continuous gap between supply and demand of organs. Nowadays, the number of people who need an organ transplant is growing significantly in comparison with the past few decades. The real problem is that the waiting list is larger than the number of donors.

Data from the U.S. Department of Health and Human Services show a big gap between the number of people in the waiting list, the transplants performed and the number of donors (figure 1). Real data show that 20 people die each day waiting for a transplant and only 3 in 1000 people die in a way that allows for organ donation.

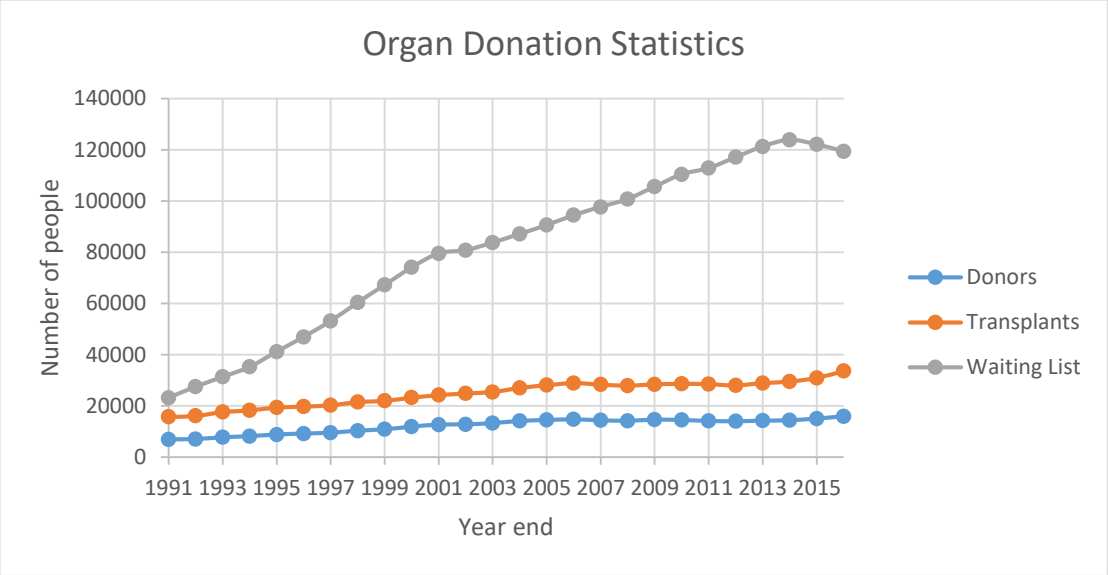

Figure 1. The big gap between the number of people in the waiting list, the transplants performed and the number of donors. (Data obtained from https://www.organdonor.gov/statistics-stories/statistics/data.html)

In order to deal with this current problem, tissue engineering (TE), which is 'an interdisciplinary field that applies the principles of engineering and life sciences toward the development of biological substitutes that restore, maintain, or improve tissue function or a whole organ' [1], is really focused in creating new or restored tissues and organs. TE wants to accomplish this goal through the use of living cells that normally are related to a matrix or a scaffold composed of natural or synthetic materials, and sometimes a composite of both.

Despite there are a lot of advances in this field and some achievements in mimicking simple structures as artificial skin, cartilage, tracheas and bladders, more work is needed in order to achieve complex structures of heterogeneous or vascularized organs and tissues [2].

Tissues and organs structures present a high structural, mechanical and biological complexity; for that reason, conventional techniques used in TE are not capable of mimicking their complexity.

The development of new biofabrication approaches tries to reach this goal, but they are still far from fabrication of functional and transplantable tissue and organs. The attempt of fabricating tissues and organs is not only addressed to implantable therapeutics, but also for their use as *in vitro* models in order to study tissue and organ development and disease, as well as tissue models for drug discovery and testing [3].

3D bioprinting is emerging more popular among biofabrication processes but it is still in its early development stages. 3D bioprinting is known as a technology that allows fabrication of 3D tissue constructs with pre-designed structures and geometries programmed by computer-aided design (CAD) [4]. The material that is used in bioprinting is termed as 'bioink'. It is a combination of biomaterials, that can be natural or synthetic, and living cells. The biomaterial provides the matrix and it can incorporate bioactive factors and some particles that will help in the viability, proliferation and differentiation of cells. There are inks that do not incorporate cells but can serve as a support, in this case they cannot receive the name of bioink.

The important difference between traditional biofabrication techniques and bioprinting is that the second one provides a high reproducibility and precise control over the tissue constructs.

2.1. 3D bioprinting technologies

As mentioned before, this new biofabrication technique contains cells in its bioink, for that reason, 3D bioprinting should be cell friendly, it means that the deposition of the ink has to be gentle in order to ensure the survival of cells. This requirement is not achieved by all common 3D printing techniques, thus limiting the number of techniques that are suitable for 3D bioprinting (figure 2).

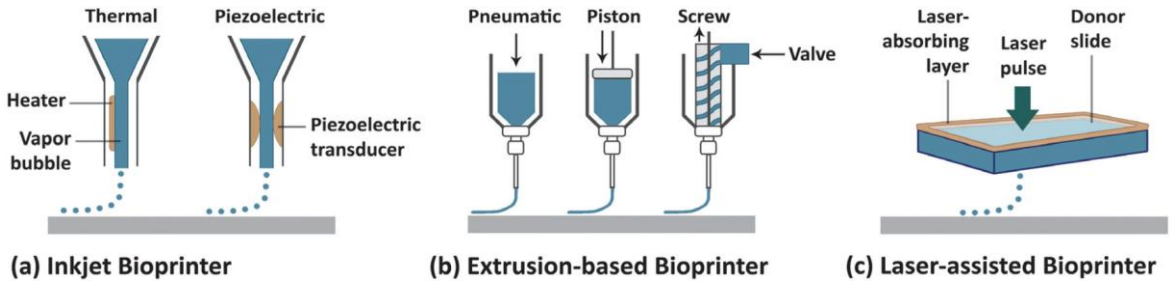

Figure 2. 3D bioprinting technologies. (a) Inkject bioprinting. (b) Extrusion-based bioprinting. (c) Laser-assisted bioprinting. [4]

- **Inkjet bioprinting** allows printing polymeric solutions, colloidal suspensions and cells suspensions with relatively low viscosities (3.5 mPa/s to 12 mPa/s) at a relatively high shear rates in the form of droplets, allowing a control of the volume and a predefined location.

  Drops of liquid are ejected due to thermal or acoustic forces. Thermal inkjet printers electrically heat the print head to produce pulses of pressure that allow the formation of droplets from the nozzle. Piezoelectric inkjet printers create an acoustic wave inside the print head that cause the breaking of the liquid into droplets, then voltage is applied to the piezoelectric material, generating the required pressure to droplets can eject from the nozzle.

  This method allows the deposition of low cell concentrations, but the cell viability after printing is >85%.

- **Extrusion-based bioprinting** allows the extrusion of high viscosity solutions (30 mPa/s to $>6 \cdot 10^7$ mPa/s), hydrogels and colloidal suspensions.

  Extrusion-based bioprinting is controlled robotically; the material is extruded and deposited in continuous beads, previously set by the CAD software. The movement of the nozzle is allowed along the *x, y* and *z* axes.

  The most common mechanisms to extrude the bioink are pneumatic or mechanical (piston or screw). Mechanically driven bioprinters have more spatial control than pneumatically driven bioprinters, which have simpler drive-mechanisms components because the force is only limited by the air-pressure.

  Extrusion-based technology allows the deposition of very high cell densities, in contrast, the cell survival is between 40% and 86%.

- **Laser-assisted bioprinting** allows the printability of biological material, such as peptides, DNA and cells.

  Focused laser penetrates on the absorbing layer of the ribbon, this ribbon is usually made of glass and covered with the laser-energy-absorbing layer (e.g. gold or titanium), to create a high-pressure bubble that impulse biological material (e.g. cells and/or hydrogel) toward the collector substrate.

  This technology allows the deposition of medium cell densities and the cell viability after printing is high.

Among the current 3D bioprinting technologies, extrusion-based bioprinting is the method that presents more advantages for the fabrication of tissue and organs constructs. Complex structures,

previously designed by CAD software, can be printed due to its high resolution; it also eases the patterning of multiple cell types.

Another important advantage is the ability to deposit very high cell densities, but with the disadvantage of a poor cell survival rate between 40% and 86% because the pressure applied when extruding the bioink from the nozzle affects cell viability due to shear stress [5].

2.2. Bioink design

By combining different bioinks and having a 3D pattern, the objective of obtaining a functional construct can be achieved (figure 3) [3].

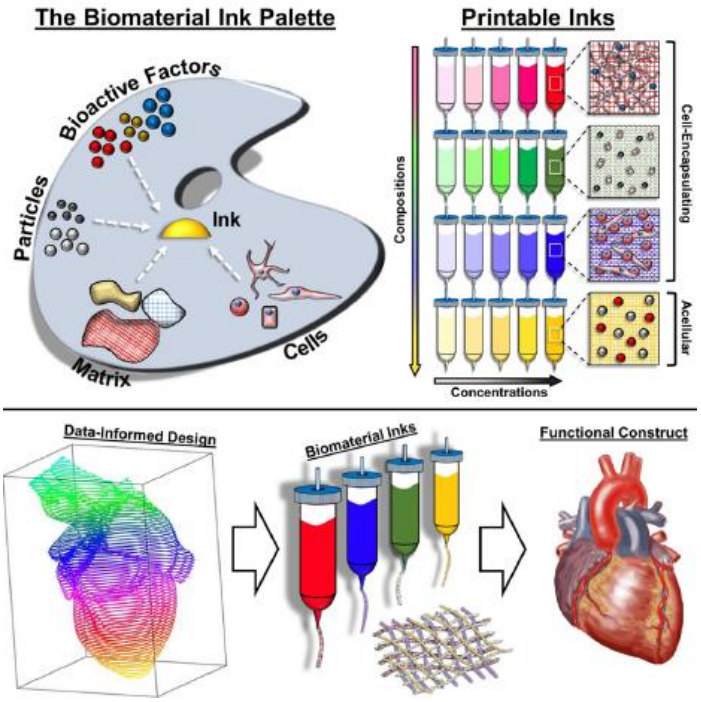

Figure 3. Schematic representation of ideal bioink composition and of the bioprinting process to create a functional construct. [3]

Bioinks are directed to specific applications depending on the type of tissue to be regenerated, the type of cells to be printed as well as the bioprinter to be used; for that reason, there are many combinations of biomaterials and cells that lead to different bioinks.

Despite all possible combinations, all bioinks must meet good requirements for bioprinting and they must possess proper bioactivity of different cell types. The requirements that an ideal bioink must meet are the following ones:

i. Creation of tissue constructs that assure a proper mechanical strength and robustness, similar to the tissue to be replaced or regenerated. These tissue constructs must incorporate scale features as biological cues to help cells to self-organize.
ii. Adjustable gelation and stabilization to provide a high reproducibility and precise control over tissue constructs. Bioink should be mechanically weak enough to be extruded, but upon extrusion the structure should maintain a 3D structure.
iii. Printability involves viscosity, surface tension and cross-linking properties of the bioink. Viscosity affects print fidelity and cell encapsulation efficiency, for that reason this parameter is important when talking about bioinks. Depending on the bioprinting technique, different viscosities are used to allow extrusion of the bioink.
iv. Biocompatibility, and, if necessary, biodegradability. Upon degradation, the bioink must not release waste products that can interfere with the natural tissue and produce inflammatory response in the host.
v. If necessary, adaptable to any chemical modification to meet tissue needs. Sometimes, functionalization of the bioink allows the incorporation of biochemical cues that help cell adhesion, migration, differentiation… [3] [4] [6]

2.3. Current bioinks

Current bioinks used for tissue and organ printing are cell-laden hydrogels, decellularized extracellular matrix (dECM)-based solutions, and cell suspensions.

Cell-laden hydrogels are the most commonly used bioinks as they have the ability to simulate the cellular microenvironment and they present tuneable properties and bioactivity by incorporating nanoparticles. This type of bioink formulation can use natural hydrogels as well as synthetic. Natural hydrogels present inherent bioactivity and they can be agarose, alginate, chitosan, collagen, gelatin, fibrin, and hyaluronic acid. On the other hand, synthetic hydrogels can be designed to enhance their biological functions. Nowadays, the more applied synthetic polymers as bioinks are pluronic (poloxamer) and poly(ethylene glycol) (PEG), or a combination of both [6].

Cell-laden hydrogels require a high viscous polymer solution for printing and rapid cross-linking to assure self-supporting structures. Hydrogels are polymer networks that retain big quantities of water due to hydrophilic groups that become hydrated in contact with aqueous media, thus allowing the formation of the hydrogel structure [7]. Cross-linking prevents the dissolution of the polymer chains and it can be physical (non-covalent), which uses hydrophobic interactions, ionic interactions and hydrogen bonding, or chemical, which relies on the formation of covalent bonds [6].

Among hydrogels used for 3D bioprinting, there are ones of special interest as they undergo a solution/gel transition upon a temperature rise, thus, giving the ability to print them in solution form while turning into gel once they reach the printing surface at the required temperature. They are named thermo-sensitive gelling systems.

Thermo-sensitive gelling systems are stable and low viscosity aqueous solutions, liquid at room temperature, that turn into a gel after an increase of temperature. They can be mixed with cells for tissue engineering applications [8].

2.4. Thermo-sensitive gelling systems based on Chitosan/Polyol-phosphate

Among the thermo-sensitive gelling systems present in literature, chitosan/polyol-phosphate (CS/PP) systems have been extensively studied in the past years [9].

CS is a biopolymer obtained by partial deacetylation of chitin, which is extracted from crustaceans' or insects' exoskeleton and from the cell walls of fungi. It is a heteropolymer composed by glucosamine units (β(1−4)-linked 2-amino-2-deoxy-D-glucose) and *N*-acetylglucosamine units (2-acetamido-2-deoxy-D-glucose).

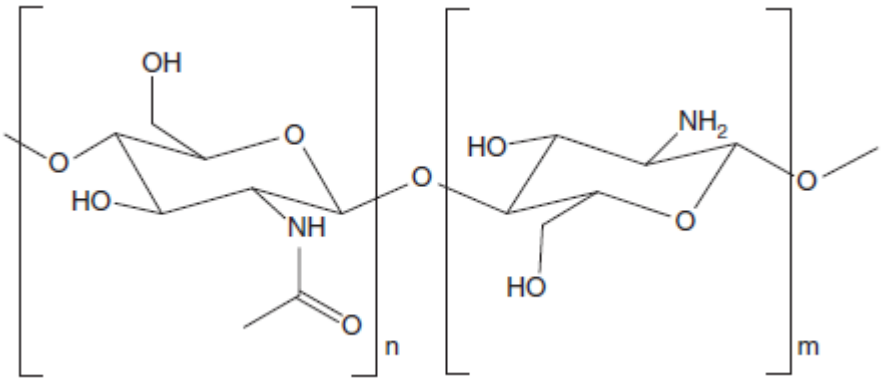

Figure 4. Chemical structure of chitosan. [9]

CS exhibits beneficial biological properties like low toxicity, biocompatibility, biodegradability, bioadhesivity and bacteriostatic effects. These properties make CS a good candidate for TE applications and also for pharmaceutical applications [8].

CS is soluble in acidic aqueous solutions, for a pH lower than the CS pK_{ap} around 6.2. In contrast, at pH higher than the pK_{ap}, the neutralization of the CS chains induces the formation of gel-like precipitates.

CS is not a thermo-sensitive polymer on its own, but Chenite *et al*., demonstrated that by the addition of glycerolphosphate (GP), CS solution becomes thermo-sensitive at physiological pH [10].

GP is an organic compound naturally found in the body. The role of GP in thermo-sensitive gelling systems is to induce the solution/gel transition at physiological pH [9].

Other studies, as the ones performed by Supper *et al.,* demonstrate that by the addition of other polyol-phosphate salts (PP) the transition from solution to gel is also possible at physiological pH [11].

The most common used PP salts as gelling agents are β-glycerolphosphate (β-GP), glucose-1-phosphate (G1-P) and glucose-6-phosphate (G6-P).

The main advantage of these systems is the absence of any organic solvents and cytotoxic agents which could affect the biocompatibility of the system and also their safety for clinical applications.

The gelation mechanism of the thermo-sensitive gelling system is still not well understood, but in 2014 Supper et *al*., [8] made a study with the objective of investigating the mechanism of gelation process. They propose an explanation of the gelation process divided in two phases:

- **Maintaining of the chitosan molecules in solution at neutral pH at low temperature.** When gelling agent is added to the solution of CS, the phosphate parts neutralize the majority of the positive charges that are present on CS. This fact causes a reduction in the charge repulsion between polymer molecules, thus inducing a formation of a gel-like precipitate. However, the presence of polyol in gelling agents prevents the polymer precipitation and the gel formation because they create a shell around the macromolecules.
  Due to hydrogen bonds formed by water molecules, glycerol and glucose create a protective hydration layer around the polymer chains. This layer prevents the formation of the gel by reducing self-interactions between CS chains because it remains stable at neutral pH and low temperature.
- **The solution/gel transition upon heating.** When increasing the temperature, there is a proton transfer from CS to the gelling agent because the proton dissociation constant of CS, pK_{ap}, is temperature-depend. This fact reduces the degree of ionization of CS and the electrostatic interactions between CS and gelling agents. There is also a reduction of the number of hydrogen bonds, decreasing the cohesion of the polyol shells around the macromolecule. As a consequence, at a $T \geq T_{S/G}$ (transition temperature from solution to gel), these facts result in the gelation of the CS/gelling agent solution.

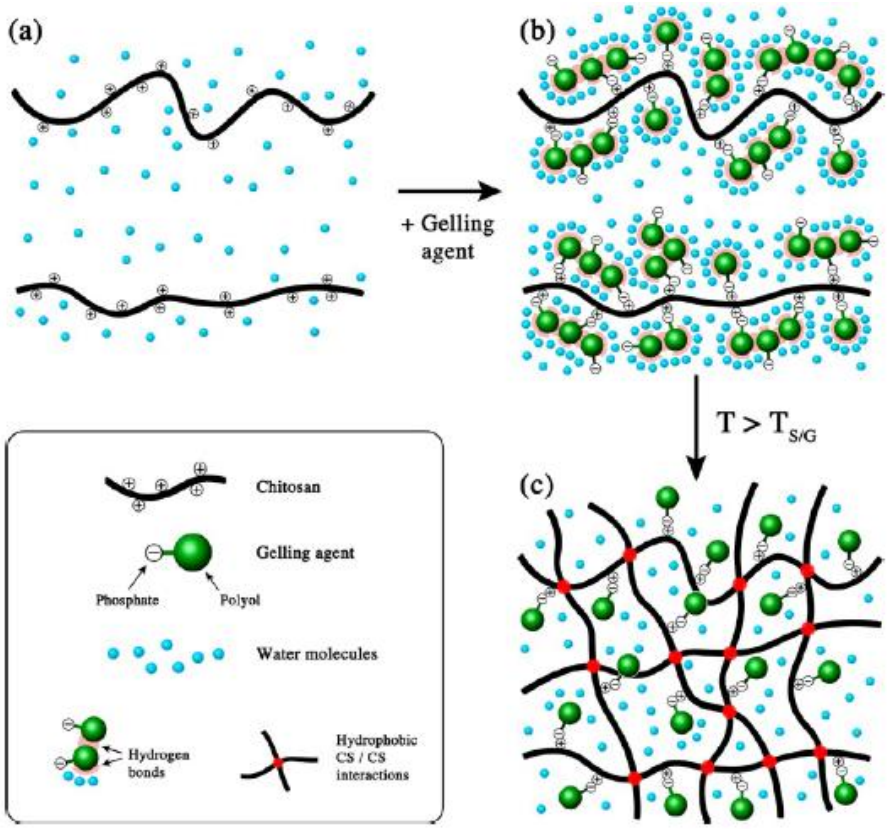

Figure 5. Gelation mechanism of the CS/GP solution. [8]

The thermo-sensitive gelling system can be affected in terms of morphology and gelation kinetics by varying some of the physico-chemical properties of the CS like the molecular weight (M_w), the deacetylation degree (DD) which is the proportion of glucosamine unit, or the distribution of glucosamine and acetylglucosamine units, or by varying also the gelling agent or the acidic solution in which the CS is dissolved. Some parameters that can be affected and the way in which they are affected are described below:

- **Gelation time and temperature.** They are crucial in thermo-sensitive gelling systems as gelation occurs at physiological temperature. These two parameters can be adjusted by varying the PP and CS ratio. Increasing the PP concentration leads to a faster gelation time, as well as increasing the CS concentration; but sometimes, increasing the CS concentration does not reduce gelation time because it also depends on the type of salt used. The polymer concentration cannot be increased sharply, otherwise, an increment of the gelation time is achieved. By using a CS of lower M_w, the gelation temperature is reduced. The increment of DD of CS also produce a reduction on the gelation time and temperature.
- **Gel strength.** This parameter is characterized by rheological analysis, through the values of the storage modulus (G') and the loss modulus (G''). G' represents the elastic behaviour of the gel, while G'' represents the viscous behaviour. CS/PP hydrogels show a strong gel behaviour if G'

is comprised between 1 and 10 kPa and G'>>G''. Gel strength can be controlled by varying the gelling agent and its concentration.

- **Storage stability.** The stability of the CS/PP solutions is mainly affected by the DD of the polymer. Also the structure of the gelling agent can affect this parameter. Gelation can also occur under storage conditions (4°C) with the pass of time [8] [9].

3. Materials and methods

3.1. Materials

Two types of chitosan (named *CS 80/100* and *95/100*) with different deacetylation degrees were used in this study, 80% and 95%, having a molecular weight average of 100 kDa and obtained from *Heppe Medical Chitosan, Germany.* Hydrochloric acid of 37% v/v was used in order to solubilize CS and it was purchased from *Merk, Austria.* Two different gelling agents were used, *β-Glycerophoshate Disodium Salt Pentahydrate* ($C_3H_7PNa_2*5H_2O$) from *Santa Cruz Biotechnology*, *USA* and *α-D-Glucose-1-Phosphate Disodium Tetrahydrate 98%* ($C_6H_{11}Na_2O_9P*4H_2O$) from *ThermoFisher, Germany*. Ultrapure water, obtained from the purification system QMillipore (*Millipore Direct Q UV3, USA*) and Dulbecco's Modified Eagle Medium (DMEM) with 2% Foetal Bovine Serum, obtained from *San Luigi Gonzaga Hospital, Orbassano (Turin), Italy,* were used in order to solubilize the gelling agent.

Phosphate-buffered saline (PBS), from *Sigma-Aldrich,* was used in order to carry out different hydrogel characterization tests. The PBS was prepared dissolving one pre-formulated tablet in 200 mL of ultrapure water.

3.2. Test groups

In order to get the thermo-sensitive hydrogel that suits better the necessities of this study, different hydrogels were tested. These hydrogel solutions were separated in four groups; as mentioned before, to obtain the thermo-sensitive solution is needed a polymer solution and a gelling agent:

- **First group:** Initial polymer solution of CS 80/100 (4.5% w/v, HCl 0.2M) and β-GP as gelling agent.
- **Second group:** Initial polymer solution of CS 80/100 (4.5% w/v, HCl 0.2M) and G1-P as gelling agent.
- **Third group:** Initial polymer solution of CS 95/100 (3.6% w/v, HCl 0.2M) and β-GP as gelling agent.
- **Fourth group:** Initial polymer solution of CS 95/100 (3.6% w/v, HCl 0.2M) and G1-P as gelling agent.

Some parameters were modified to see how they affect to the hydrogels' properties:

- The concentration of CS in weight volume (% w/v) in the final solution of CS/PP. This parameter affects by varying the volume of ultrapure water or DMEM used to solubilize the salt.
- The amount of salt (in grams) within a known volume of CS solution.

- The solubilisation of the gelling agent in ultrapure water or DMEM.

From a previous master thesis [12], calculations were obtained in order to know the exact amount of gelling agent that has to be mixed with ultrapure water or DMEM and to be added to CS.

This amount of gelling agent varies depending on the number of mol of amino groups (NH_2) present in the polymer chain. Therefore, it had to be added a number of mol of gelling agent (GA) equal or superior to the number of mol of NH_2 present in the CS, according to this equation:

$$\boldsymbol{mol_{GA} = R \cdot mol_{NH2}} \qquad \textbf{(Eq. 3.1)}$$

Where mol_{GA} are the mol of the gelling agent salt and mol_{NH2} are the mol of NH_2 of the CS, both in a known volume, and R is the ratio between both.

A polymer is characterized by its degree of polymerization, which is the number of monomeric units in a polymer. The degree of polymerization was necessary to know the number of amino groups present in the polymer, knowing the molecular weight of the polymer (M_w polymer) and the molecular weight of a monomeric unit (M_w monomeric unit).

$$\boldsymbol{polymerization\ degree = \frac{M_w\ polymer}{M_w\ monomeric\ unit}} \qquad \textbf{(Eq. 3.2)}$$

The CS used in this study had a molecular weight average of 100 kDa. Considering a deacetylation degree of 100% and taking into account that the molecular weight of a monomeric unit is 189.215 g/mol, the polymerization degree is 528 for a CS of 100/100. As the two types of CS which were being studied were CS 80/100 (80% deacetylation degree) and CS 95/100 (95% deacetylation degree), their respective polymerization degrees were 422 and 501.

In order to calculate the number of chains present in a known volume of CS solution, it was necessary to know first the amount of CS present in this known volume of solution. For example, taking a volume of 1 mL, for CS 80/100 at 4.5% w/v the milligrams of CS were 45 mg; while for CS 95/100 at 3.6% w/v the milligrams of CS were 36 mg. At this point, calculating the weight of a chain by relating the Avogadro's number (~$6.022 \cdot 10^7$) with the molecular weight of the CS, and multiplying by the amount of the CS present in 1 mL, the number of chains was gotten. For CS 80/100 the number of chains was $2.7099 \cdot 10^{17}$, while for CS 95/100 the number of chains was $2.1679 \cdot 10^{17}$.

Knowing the number of polymer chains present in a known volume of CS, it was possible to get the number of amino groups and the number of mol of NH_2 in the known volume. For a volume of 1 mL of

CS, the correspondent number of mol of NH_2 were $190.2 \cdot 10^{-6}$ for CS 80/100 and $180.4 \cdot 10^{-6}$ for CS 95/100.

Thus, following the equation 3.1., the number of mol of gelling agent was known. Then, multiplying this number by the molecular weight of the gelling agent (M_w GA) that were 306.12 g/mol for β-GP and 376.172 g/mol for G1-P, the mass of gelling agent needed was calculated.

Different concentrations of both polymer and salt were chosen on the basis of the results obtained from a previous master thesis [12] that studied CS/β-GP solutions.

Hence, for the first group, CS 80/100 (4.5% w/v, HCl 0.2M) and β-GP, CS/β-GP solutions, using ultrapure water as salt solvent, were obtained at a final concentration of CS of 1.5% w/v and different R (4, 5, 6, 7, 8). Successively, CS/β-GP solutions, using DMEM as salt solvent, were obtained at a final concentration of CS of 1.5% w/v and R equal to 8.

For the second group, CS 80/100 (4.5% w/v, HCl 0.2M) and G1-P, CS/G1-P solutions, using ultrapure water as salt solvent, were obtained at a final concentration of CS of 1.5% w/v and different R (5, 7).

For the third group, CS 95/100 (3.6% w/v, HCl 0.2M) and β-GP, CS/β-GP solutions, using DMEM as salt solvent, were obtained at a final concentration of CS of 2.5% w/v and R equal to 4.

For the fourth group, CS 95/100 (3.6% w/v, HCl 0.2M) and G1-P, CS/G1-P solutions, using ultrapure water as salt solvent, were obtained at a final concentrations of CS of 2.5% w/v with R equal to 2.5 and 3, 2% w/v with R equal to 2.5, 3, 3.5, 4 and 4.5, and 1.75% w/v with R equal to 4.5. Successively, CS/G1-P solutions, using DMEM as salt solvent, were obtained at a final concentration of CS of 2% w/v and R equal to 4.5.

3.3. Preparation of CS/PP solution

The incoming procedure was followed to prepare the CS/PP solution in order to get the hydrogel. Two separated solutions (one for CS and the other for the selected PP salt) were prepared to be mixed at the end of the procedure.

On the one hand, a solution of CS and HCl was prepared. As mentioned before, two types of CS were used, CS 80/100 and CS 95/100; depending on the type of CS used, different concentrations were taken into account: 4.5% w/v for CS 80/100 and 3.6% w/v for CS 95/100. Chitosan is a powder that has to be solubilized in HCl to obtain a solution. The polymer powder was dissolved into HCl 0.2 M with the help of a magnetic stirrer (*RCT safety control, IKA*) always inside a fume hood (*Typhoon, Labosystem*), during 48 h and at environmental temperature. The solution was stored in the fridge at ~4°C.

On the other hand, gelling agent solutions were prepared mixing the desired polyol-phosphate salt (β-GP and G1-P) and ultrapure water or DMEM that were added by the aid of a micropipette of 100-1000 µL (*Pipetman, Gilson*). In literature [11], it is found that gelling agent is dissolved in ultrapure water, but it was also tested dissolving the gelling agent in DMEM, which is a cell culture medium used to maintain most types of cells. The reason of that was to create a better environment for cells to grow, as the hydrogel would be designed to incorporate cells.

Several problems appeared when mixing the gelling agent and DMEM, and the most important one was the appearance of bubbles in the solution when both were mixed using a vortex mixer due to high rpm; the bubbles disturbed the homogenization. To avoid the bubbles, the solution was mixed using a magnetic stirrer. On the contrary, when mixing ultrapure water with the gelling agent there was no problem of bubbles and the solution was mixed using a vortex mixer (*ZX3, VELP Scientifica*) at high rpm.

Another important factor was the control of the increase of volume when adding the media to the PP salt, as the salt is hydrated and releases water. For that reason, the addition of DMEM was controlled using a graduated cylinder. The pH of this PP solution was measured.

In order to get the CS/PP solution, a series of steps was followed. First of all, the required volume of CS depending on the desired final concentration was taken from the previous prepared CS solution using a pipette. The sample was maintained in the fridge overnight to eliminate the presence of air bubbles that appeared when the sample volume was taken.

Gelling agent solution was added to CS solution dropwise, introducing the CS solution into an ice-bath to maintain a temperature between ~4°C – 6°C and under magnetic stirring to mix the final solution. This step was very important in order to obtain homogenization of the solution and no apparition of precipitates. After mixing, the solution was further stirred for another ~10min. The final pH of the solution was measured.

Once the CS/GP solution was prepared, it was stored in the fridge at ~4°C.

3.4. Characterisation of hydrogels

3.4.1. Gelation time

The gelation time was defined as the time at which the CS/PP solution becomes a hydrogel. In order to know this approximated value, Test Tube Inversion Method [9] was used (figure 6). When Test Tube Inversion Method is performed, the gelation time corresponds to the time at which the CS/PP sample does no longer flow after incubation at a given temperature.

0.5 mL of CS/GP solution were introduced in an Eppendorf of 1.5 mL by the aid of a micropipette of 500-5000 µL (*Pipetman, Gilson*). The Eppendorf was placed in the incubator (*CoolSafe, SCANVAC*) at ~37°C. At different intervals of time, 2 or 3 min at the beginning, the sample was taken out from the incubator and overturned to see if the solution flowed by its own weight following the procedure of the Test Tube Inversion Method.

If the solution flowed, the sample was introduced again in the incubator for another minutes. This time was decided depending on how the solution was; if it was very liquid, the waiting time was higher. If the solution did not flow, it meant that the solution had become a hydrogel.

This method was applied to all groups of CS/PP solution in order to know the gelation time of each sample, it means, it was applied to all different concentrations and ratios of CS 80/100 with β-GP, CS 80/100 with G1-P, CS 95/100 with β-GP and CS 95/100 with G1-P.

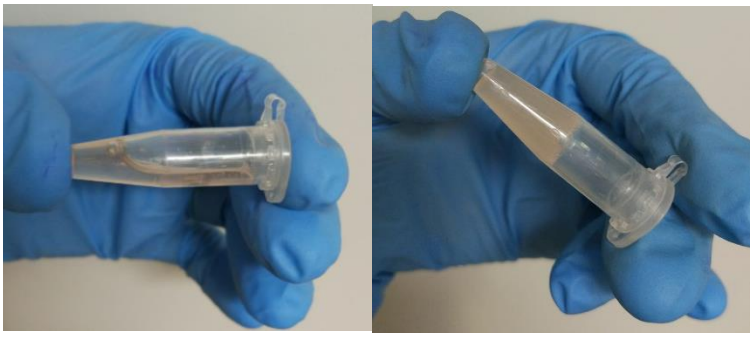

Figure 6. Test Tube Inversion Method.

3.4.2. pH measurements

pH was an important parameter to be controlled in this study due to the viability of cells. As one of the purposes of the hydrogel is to encapsulate cells, the pH had to be in the range of 7.0 - 7.4 [13].

Two different measurements of pH were done. One of them was the measure of the pH of each CS/PP solution, which was applied to all different concentrations and ratios of CS 80/100 with β-GP, CS 80/100 with G1-P, CS 95/100 with β-GP and CS 95/100 with G1-P. The other was the measure of the pH during the gelation process, and it was only applied to those solutions that showed a better behaviour and characteristics for bioprinting; they were CS 95/100 2.5% w/v R=4 with DMEM and β-GP, and CS 95/100 2% w/v R=4.5 with DMEM and G1-P.

In order to control the pH during the gelation process, 0.5 mL of CS/GP solution were introduced in an Eppendorf of 1.5 mL by the aid of a micropipette of 500-5000 µL. The pH was measured with a pH-meter (*HI 9124/25 pH-meter, Hanna Instruments, Italy*), using a glass electrode, which is more precise. The glass electrode was placed in the Eppendorf, touching the solution, and both were introduced in the incubator at ~37°C.

Subsequently, the pH was monitored at intervals of 15 secs, 30 secs, 60 secs and 120 secs until the pH was stable for several minutes.

3.4.3. Degradation test

The purpose of the degradation test was to see the degradation of the hydrogel at 37°C when it is in contact with a buffer solution that simulates the extracellular fluid present in mammals. This buffer solution is PBS, phosphate-buffered saline, and its pH is 7.4.

Two types of degradation tests were performed. The degradation test was performed only on optimal CS/PP solutions (see paragraph 4.1.). The first test was using PBS as buffer solution and it was performed with CS 95/100 2.5% w/v R=4 with DMEM and β-GP, CS 95/100 2% w/v R=4.5 with DMEM and G1-P, and CS 80/100 1.5% w/v R=8 with DMEM and β-GP. To further investigate the degradation of the CS/PP hydrogels, a second test was performed adding lysosome to PBS. Lysosome is an enzyme characterized by the degradation of polymers. The concentration of lysosome was 1 mg/mL of PBS. Thus, the second test was done with CS 95/100 2.5% w/v R=4 with DMEM and β-GP, and CS 95/100 2% w/v R=4.5 with DMEM and G1-P.

In order to do the test, 15 samples of each CS/PP solution were prepared. ~0.8 mL of solution were placed in polystyrene bijous (diameter of 18 mm, volume of 7 mL, *Thermo Scientific™ Sterilin™*) and incubated at 37ºC during 1 hour to ensure gelation.

When the hydrogel was formed ~1.6 mL of PBS solution (with or without lysosome), previously warmed at 37ºC in the incubator, were added to each bijou. The samples were introduced again into the incubator.

After various intervals of time, 1 hour, 1 day, 5 days, 7 days and 14 days, 3 samples were taken out from the incubator. PBS solution previously added to each sample was poured into a new polystyrene bijou in order to measure the pH. The weight of the hydrogel (W_{wet}) was measured after removing all the presence of PBS with the help of an absorbent sheet of paper. After that, the samples were introduced into the freezer in order to proceed with lyophilisation. The samples were lyophilised with a freeze dryer (*Scanvac, CoolSafe™, Denmark*) for 24 hours and then, the weight (W_{lyo}) was measured again.

Hence, the Equilibrium Water Content (EWC) was calculated as:

$$\boldsymbol{EWC}(\%) = \frac{\boldsymbol{W_{wet} - W_{lyo}}}{\boldsymbol{W_{wet}}} \cdot \mathbf{100} \qquad \textbf{(Eq. 3.3)}$$

And the Weight Loss (WL) was calculated as:

$$\boldsymbol{WL}(\%) = \frac{\boldsymbol{W_{lyo\_Exp}} - \boldsymbol{W_{lyo}}}{\boldsymbol{W_{lyo\_Exp}}} \cdot \mathbf{100} \qquad \textbf{(Eq. 3.4)}$$

Where W_{lyo_Exp} was the weight of 0.8 mL of hydrogel after lyophilisation, without the addition of PBS.

3.4.4. Kaiser test

The Kaiser test is colorimetric test useful for the detection of free amino groups. This test was applied to PBS plus lysosome solution that was added in the degradation test (see paragraph 3.4.3.), to see if lysosome had degraded the CS of the hydrogel, thus, liberating free amino groups to PBS plus lysosome solution.

The test was done with a Kaiser test kit from *Sigma-Aldrich*. PBS plus lysosome solution that was tested came from the degradation test of two hydrogels, CS 95/100 2% w/v R=4.5 with DMEM and G1-P, and CS 95/100 2.5% w/v R=4 with DMEM and β-GP.

First of all, 250 µL of the extracted PBS plus lysosome solution that was added to the hydrogel in the degradation test were introduced in a small vial of 1.5 mL of volume with the aid of a micropipette of 100-1000 µL (*Pipetman, Gilson*).

Then, with a micropipette of 10-100 µL (*Pipetman, Gilson*), correspondent volumes of the Kaiser kit's solutions were added:

- 75 µL of phenol, 80% in ethanol.
- 100 µL of KCN in H_2O/ pyridine.
- 75 µL of Ninhydrin, 6% in ethanol.

The samples were slightly shaked and then introduced in an oven at 120°C for 5 minutes.

Later, 100 µL of each vial were extracted and poured into a microplate with a micropipette of 10-100 µL. The microplate was introduced into a microplate reader (*Multimode Plate Reader VICTOR X3, Perkin Elmer*). The microplate reader was used for absorbance detection. A light source illuminated the sample using a blue wavelength and a light detector located on the other side measured how much of the initial light was transmitted through the sample. Thus, the amount of transmitted light was related to the concentration of free amino groups.

3.4.5. Rheological measurements

Rheological measurements were used to assess the deformation and flow behaviour of the CS/PP hydrogels. Seven types of tests were performed with a rheometer (*Modular Compact Rheometer 302, Anton Paar*).

In order to have a better comprehension of the performed rheological tests, some parameters need to be defined.

- **Shear stress τ** (in Pa, Pascal): shear force F (in N, Newton) applied per unit area A (in m^2).

$$\tau = \frac{F}{A_0} \qquad \textbf{(Eq. 3.5)}$$

Figure 7. Shear stress is the force moving the upper plate divided by the plate's area [14].

- **Shear rate Ϋ** (in 1/s): velocity v (in m/s) divided per shear gap h (in m).

$$\dot{\gamma} = \frac{v}{h} \qquad \textbf{(Eq. 3.6)}$$

Figure 8. Shear rate is the velocity of the moving plate divided by the distance between the plates [14].

- **Viscosity η** (in Pa·s): all liquids are composed of molecules and some particles. When put into motion, molecules and particles are forced to slide along each other and they develop a flow resistance caused by internal friction [14]. In order to measure this flow resistance when internal friction is applied, viscosity is represented as shear stress τ (in Pa, Pascal) divided per shear rate Ϋ (in 1/s).

$$\eta = \frac{\tau}{\dot{\gamma}} \qquad \textbf{(Eq. 3.7)}$$

- **Shear strain ϒ** (dimensionless, usually expressed as percentage): deflection path s (in m) divided per shear gap h (in m).

$$\Upsilon = \frac{s}{h} \qquad \textbf{(Eq. 3.8)}$$

- **Storage Modulus G'** (in Pa, Pascal): represents the elastic behaviour of the material.
- **Loss Modulus G''** (in Pa, Pascal): represents the viscous behaviour of the material.

Two types of solutions were studied in these test, the CS/G1-P solution with a final concentration of CS 95/100 at 2% w/v for a R=4.5 with DMEM, and the CS/β-GP solution with a final concentration of CS 95/100 at 2.5% w/v for a R=4 with DMEM.

The Shear Strain Test was done in order to know at which value of the shear strain amplitude can be performed the following tests to ensure that all measurements were carried out within the viscoelastic range. This value is known when G' and G'' are linear and parallel. Before starting the test, the temperature was set at 37 °C and waited for 30 minutes to ensure gelation of the hydrogel. During the test, the temperature was maintained at 37°C and the rotational oscillation (shown in Figure 9) was set at a frequency of 1 Hz while shear strain was varying.

The Ramp Sweep Test was done in order to know how the viscosity of the hydrogel varies while temperature is increasing at a certain rate. The continuous rotation (shown in Figure 9) was set at a shear rate of 1 s^{-1}. The range of temperature was from 0 °C to 50 °C. Different Ramp Sweep Tests were performed at rates of 0.5, 1, 1.5 and 2 °C/min.

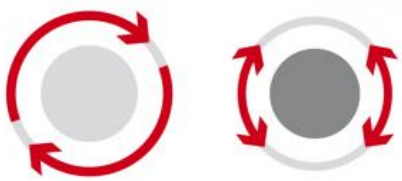

Figure 9. Left: Continuous rotation, right: rotational oscillation [14].

The Time Sweep Test was done in order to know at which exact time the solution becomes a hydrogel. This value is known when G' and G'' cross. The rotational oscillation was set at a frequency of 1 Hz and a shear strain amplitude of 1% (extracted from the results of the Shear Strain Test). Before starting the test, the temperature was set at 37 °C and waited for 30 minutes to ensure gelation of the hydrogel. The temperature was constant during the test at the same value.

The Temperature Sweep Test was done in order to know at which exact temperature the solution becomes a hydrogel. This value is known when G' and G'' cross. The rotational oscillation was set at a

frequency of 1 Hz and a shear strain amplitude of 1%. The range of temperature was from 0 °C to 50 °C. Temperature Sweep Tests were performed at a rate of 1.5 °C/min.

Thixotropic behaviour is a property that some fluid materials exhibit. They become less viscous upon application of stress or shear rate. Then, upon ceasing the shear rate, the material recovers its viscosity. This phenomenon is caused by the breakdown of the internal network structure when shear rate is applied, then, the material requires time to rebuild its structure [15].

In order to characterize the thixotropic behaviour of the hydrogel, the following test was done. The test was divided in four phases whose parameters are shown in the following table (table 1):

Phase	**Rotational oscillation**	**Continuous rotation**	**Rest**	**Rotational oscillation**
Shear strain, ϒ [%]	1			1
Frequency, f [Hz]	1			1
Shear rate, $\dot{\gamma}$ [s^{-1}]		1	0	
Temperature, T [°C]	37	37	37	37

Table 1. Parameters used in the thixotropic test.

The first phase of rotational oscillation showed G' and G'' without the application of shear rate; oscillation at very low shear strain is applied in order to simulate the behaviour at rest. In the second phase, continuous rotation at high shear rate was applied in order to simulate the internal breakdown of the structure, showing the change in viscosity. Then, one phase of rest was needed, where the hydrogel was supposed to recover its internal structure. The test ended with another phase of rotational oscillation at very low shear strain to simulate structural regeneration at rest and to compare the values of G' and G'' with the ones belonging to the first phase.

The sixth test that was performed with the rheometer was the characterization of the Viscosity versus Shear Rate. This test was needed to see the behaviour of the viscosity due to the application of different shear rates. In this test, different continuous rotations were applied to the hydrogel by varying the values of shear rate from 0.1 to 100 1/s with a rate of 5 pt./dec. Before starting the test, the temperature was set at 37 °C and waited for 30 minutes to ensure the gelation of the hydrogel. The temperature was constant during the test at the same value.

The Frequency Sweep Test was performed at different temperatures, at 20°C, 30°C and 37°C. G' and G'' were measured over angular frequencies (ω), from 0.1 to 100 rad/s, increasing through logarithmic steps. Before starting the test, the temperature was set at the proper value and waited for 30 minutes

to ensure stabilization. The strain amplitude was set at 1% along the entire test. This test was useful to know the behaviour of the solution/gel transition at different temperatures while increasing rotational oscillation was applied.

3.5. Bioprinting

For this study, experiments of bioprinting were done with a 3D bioprinter (*INKREDIBLE + 3D Bioprinter, CELLINK*). This model is quite new in the market and it allows to print human tissue; it also offers excellent accuracy, high reproducibility, and ease of use. The bioprinting technology that the bioprinter uses is extrusion-based bioprinting and the mechanism to extrude the bioink is pneumatic, the force is provided by air pressure.

The mechanism of this bioprinter was quite simple and the most important used components where:

1. On/Off Button
2. Heated printhead 1 (Ph 1)
3. Heated printhead 2 (Ph 2)
4. Printbed
5. Digital pressure monitor for printhead 1
6. Digital pressure monitor for printhead 2
7. SD-card reader
8. Control knob
9. Main LCD display
10. Cartridge air connector for printhead 1
11. Cartridge air connector for printhead 2
12. Pressure regulator for printhead 1
13. Pressure regulator for printhead 2

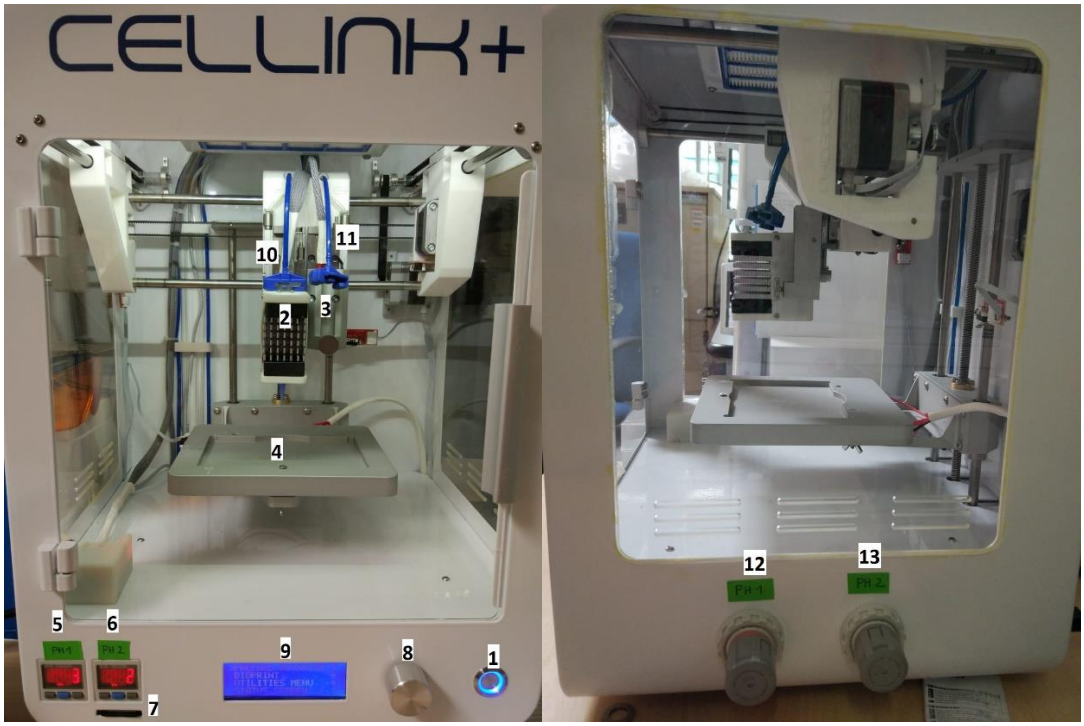

Figure 10. Left: frontal view of the bioprinter. Right: Right side view of the bioprinter. Important components are numbered.

The air pressure needed to extrude the bioink was provided by an air compressor (*Airbrush Kompressor AF18-2, ARTIKEL 34203, Wiltec*).

The bioprinter also incorporated UV-LED to crosslink bioprints, but in this study, UV-LED was not used.

Experiments were done with printhead 1; printhead 2 was deactivated. The inks used in this study were the CS/PP solutions, in solution form, semi-hydrogel form or hydrogel form. Ink was manually loaded in a syringe with a nozzle at the end and both were inserted in printhead 1.

Before using the bioprinter, calibration in *x, y* and *z* axes was needed. Calibration in the *x* and *y* axes was done by the bioprinter and calibration in the *z* axis was done manually.

The temperature of the printbed could be controlled and the value was set manually depending on the ink that was going to be tested. The temperature of the printhead could be also controlled.

All patterns that the bioprinter could print were stored in a SD-card. These patterns were previously designed by CAD and then passed to the format .gcode, the format that the bioprinter is able to read. The .gcode format provides all the instructions to the bioprinter, as well as, the movements in the *x*, *y* and *z* axes, and when the printhead has to be opened or closed.

After loading the ink in the syringe, calibrating the bioprinter and selecting the desired temperature for the printbed and the printead, the pattern was selected and bioprinter started to print.

Some previous parameters were decided:

- **State of the ink**. The ink was decided to be printed in solution form, semi-hydrogel form and hydrogel form.
    - For solution form, solution of CS/PP was loaded in the syringe and extruded, once it reached the surface of the Petri dish at 37°C, solution/gel transition took place.
    - For semi-hydrogel form, solution of CS/PP was loaded in the syringe and put in the incubator for a time shorter than gelation time of each solution to assure a semi-hydrogel state. Once the semi-hydrogel reached the surface of the Petri dish at 37°C, it finally converted in hydrogel.
    - For the hydrogel form, solution of CS/PP was loaded in the syringe and put in the incubator for a time equal or bigger than gelation time of each solution to assure a hydrogel state. Hydrogel was directly printed.
- **Addition of PBS solution.** In some cases, PBS solution was added to the Petri dish covering its entire surface to study if this fact changed the final printed appearance.

Other parameters that depended on the bioprinter were adjusted in order to find the best conditions to print the ink that was being investigated. These parameters were:

- **Diameter of the nozzle**. Different diameters were available and they were 22 G, 25 G and 27 G and their respective colours to differentiate them were blue, red and white.
- **Temperature of the printbed.** Normally the printbed temperature was set at 40°C to assure that the surface of the Petri dish that was placed on the printbed was at 37°C, the temperature at which the solution/gel transition takes place.
- **Temperature of the printhead.** This was the temperature at which the syringe that contained the ink was maintained. Two temperatures were used, one at 0°C when the hydrogel was printed in solution form, and other at 37°C when the hydrogel was printed in semi-hydrogel or hydrogel form.
- **Pressure.** Different pressures were set in order to extrude the ink. Pressure varied for each ink depending on the state of the ink and the diameter of the nozzle used but the range was normally between 8 kPa and 20 kPa.

Experiments with optimal hydrogels were performed (see paragraph 4.3.), one of them was the CS/G1-P solution with a final concentration of CS 95/100 at 2% w/v for a R=4.5 with DMEM, and the other was the CS/β-GP solution with a final concentration of CS 95/100 at 2.5% w/v for a R=4 with DMEM.

Different combinations of the before mentioned parameters were tried in order to achieve the best conditions. The printed structure was a grid of two layers.

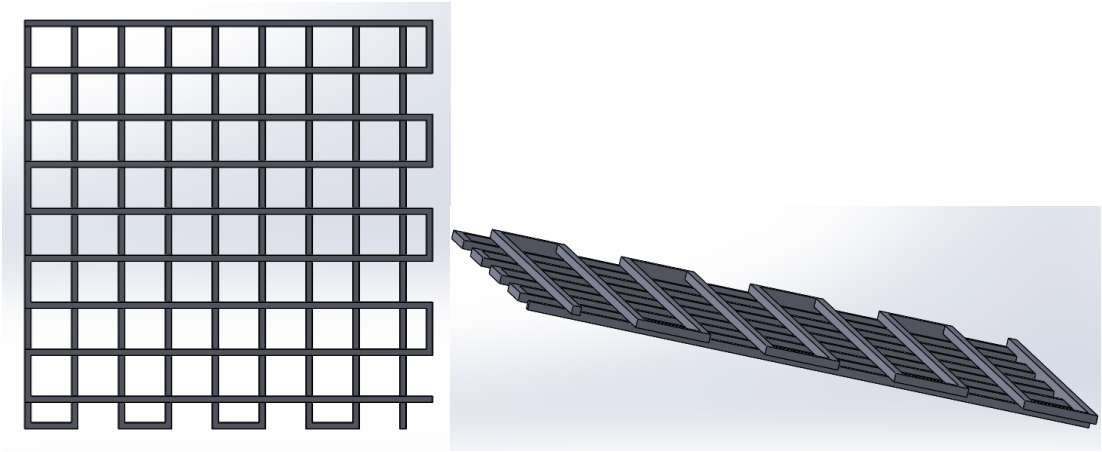

Figure 11. Grid of two layers, different views.

These combinations depended on the state of the ink, the diameter of the nozzle and the addition or no addition of PBS solution as it is represented in the following scheme. The temperature of the printbed was always set at 40°C and the pressure varied depending on the ink.

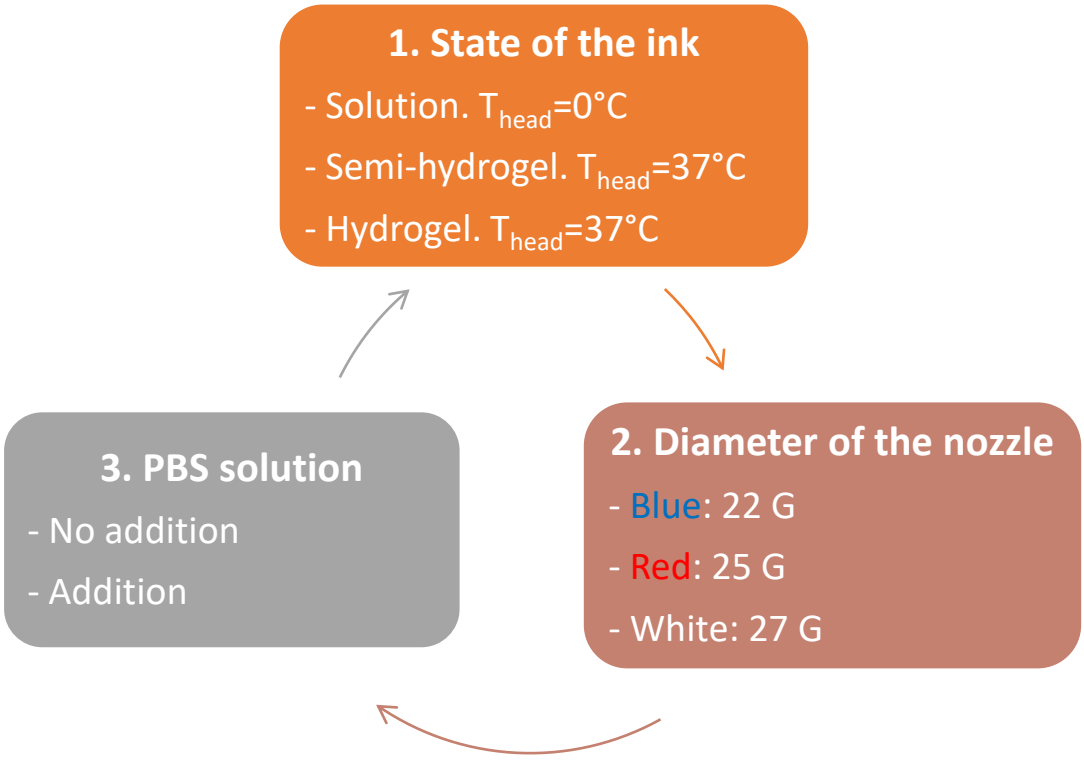

Figure 12. Decision of printing parameters.

Once all the previous parameters were tested, the combinations that gave better results were selected. With these combinations of parameters, a more complex structure was tried to be printed, in that case it had 4 layers, in order to see if the hydrogel maintained its structure in a 3D form.

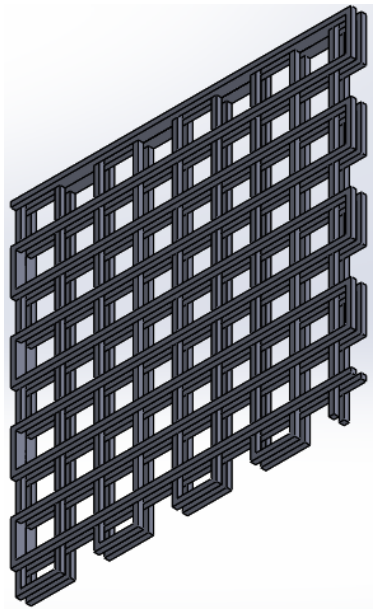

Figure 13. Grid of four layers.

Then, if good results were achieved with the grid of 4 layers, another complex structure of 8 layers was tried to be printed.

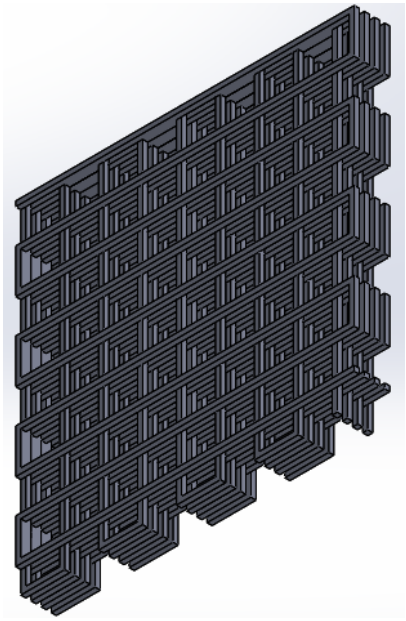

Figure 14. Grid of eight layers.

3.6. Statistical analysis

The statistical analysis of the results obtained from the tests was done with the Excel version 2016 for Windows (*Microsoft Software*). In graphs, experimental values were reported as the average values ± standard deviation.

4. Results and discussion

4.1. Gelation time and pH

The following gelation times were measured for a volume of 0.5 mL of CS/PP solution at 37°C.

For the first group of hydrogels, CS 80/100 (4.5% w/v, HCl 0.2M) and β-GP, different gelation times (table 2) were achieved by varying the R or the gelling agent solvent in which the salt was dissolved. Results showed that an increase in the gelling agent concentration leads to a decrease in the gelation time and to an increase in the pH. The best result, using ultrapure water, was achieved with CS 80/100 at a final concentration of 1.5% w/v and R equal to 8, for that reason, it was tested again with DMEM instead of ultrapure water as gelling solvent. It was observed that DMEM decreased the gelation time of the solution, in this case from 13 minutes to 5 minutes, achieving the lowest gelation time in this group of hydrogels. DMEM also reduced the pH of the final solution, in this case from 7.69 to 7.42.

Taking into account the gelation time, CS 80/100 dissolved in β-GP at a final concentration of 1.5% w/v, R equal to 8 and DMEM was considered a good candidate for bioprinting.

First group: CS 80/100 (4.5% w/v, HCl 0.2M) and β-GP				
Final solution concentration (% w/v)	**R**	**Gelling agent solvent**	**T_{gel} (min)**	**pH**
1.5	4	Ultrapure water	∞	7.3
1.5	5	Ultrapure water	20	7.35
1.5	6	Ultrapure water	18	7.5
1.5	7	Ultrapure water	15	7.56
1.5	8	Ultrapure water	13	7.69
1.5	8	DMEM	5	7.42

Table 2. Gelation times for CS 80/100 (4.5% w/v, HCl 0.2M) and β-GP.

For the second group of hydrogels, CS 80/100 (4.5% w/v, HCl 0.2M) and G1-P, the same concentration and two different R were tested in order to compare the behaviour of the gelling agent. Concentration

of 1.5% w/v and R equal to 5 and 7 were selected (table 3), taking into account previous results with CS 80/100 and β-GP.

Using G1-P as gelling agent caused an increment in gelation time, thus, leading to gelation times that were not suitable for bioprinting conditions. It also caused a decrease in the pH of both solutions.

Second group: CS 80/100 (4.5% w/v, HCl 0.2M) and G1-P				
Final solution concentration (% w/v)	**R**	**Gelling agent solvent**	**T_{gel} (min)**	**pH**
1.5	5	Ultrapure water	90	7.4
1.5	7	Ultrapure water	60	7.37

Table 3. CS 80/100 (4.5% w/v, HCl 0.2M) and G1-P.

From a previous master thesis [12], the best result of gelation time for CS 95/100, β-GP and ultrapure water was achieved at a final concentration of 2.5% w/v and R equal to 4, and it was 5 minutes. In this study, the same concentration and R were tested but using DMEM as gelling agent solvent. In this case, the result in gelation time was the same, 5 minutes.

Third group: CS 95/100 (3.6% w/v, HCl 0.2M) and β-GP				
Final solution concentration (% w/v)	**R**	**Gelling agent solvent**	**T_{gel} (min)**	**pH**
2.5	4	DMEM	5	7.11

Table 4. CS 95/100 (3.6% w/v, HCl 0.2M) and β-GP.

So, taking into account the gelation time, CS 95/100 dissolved in β-GP at a final concentration of 2.5% w/v, R equal to 4 and DMEM was considered a good candidate for bioprinting.

For the fourth group of hydrogels, CS 95/100 and G1-P, different final concentrations and R were tested (table 5). Starting with a final solution concentration of 2.5% w/v, the gelation times were high and not suitable for bioprinting. Lowering the final solution concentration to 2%, the gelation time decreased; and increasing the R and maintaining the same concentration, the gelation time decreased more. Values of pH varied and were not proportional to the concentration of gelling agent.

Observing this behaviour of the hydrogel, that was the decrease in gelation time by lowering the final solution concentration and increasing the R, it was decided to test CS 95/100 at a final concentration of 1.75% w/v and R equal to 4.5. Gelation was not achieved at this concentration and R.

Hence, the best result, using ultrapure water, was achieved with CS 95/100 at a final concentration of 2% w/v and R equal to 4.5, for that reason, it was tested again with DMEM instead of ultrapure water as gelling solvent. It was observed that DMEM decreased the gelation time of the solution in this case from 12 minutes to 10 minutes, achieving the lowest gelation time in this group of hydrogels. The pH was reduced from 7.2 to 7.02.

Taking into account the gelation time, CS 95/100 dissolved in G1-P at a final concentration of 2% w/v, R equal to 4.5 and DMEM was considered a good candidate for bioprinting.

Fourth group: CS 95/100 (3.6% w/v, HCl 0.2M) and G1-P				
Final solution concentration (% w/v)	**R**	**Gelling agent solvent**	**T_{gel} (min)**	**pH**
2.5	2.5	Ultrapure water	180	7.08
2.5	3	Ultrapure water	70	7.22
2	2.5	Ultrapure water	85	7.17
2	3	Ultrapure water	35	6.99
2	3.5	Ultrapure water	25	7.21
2	4	Ultrapure water	20	6.96
2	4.5	Ultrapure water	12	7.2
1.75	4.5	Ultrapure water	∞	7.31
2	4.5	DMEM	10	7.02

Table 5. CS 95/100 (3.6% w/v, HCl 0.2M) and G1-P.

Hence, the best candidates for bioprinting were selected regarding the lowest gelation time and a pH in the physiological range of 7.0-7.4 [13]:

- CS 80/100 dissolved in β-GP at a final concentration of 1.5% w/v, R equal to 8 and DMEM.
    - T_{gel} = 5 minutes
    - pH = 7.42
- CS 95/100 dissolved in β-GP at a final concentration of 2.5% w/v, R equal to 4 and DMEM.
    - T_{gel} = 5 minutes
    - pH = 7.11
- CS 95/100 dissolved in G1-P at a final concentration of 2% w/v, R equal to 4.5 and DMEM.
    - T_{gel} = 10 minutes
    - pH = 7.02

Therefore, it was demonstrated that the variation of some parameters in the formulation of the solution affected the gelation time and the pH. The stability of the solution was also affected by the variation of parameters.

The stability of CS/PP solutions is a critical parameter that needs to be observed to ensure an acceptable permanence of the solution before its use. Solution/gel transition occurs not only upon increasing the temperature but also with the time under storage conditions [9].

It was observed that stability of solutions was mainly affected by the DD of the polymer and the gelling agent used in each solution.

Generally, stability at room temperature (~24-27°C) was bad and the solution converted in hydrogel in less than 3 hours.

When using CS 80/100 and β-GP the stability time at refrigerated temperature (~4-6°C) was higher than when using CS 95/100 and the same gelling agent, it means that CS 80/100 took more time to achieve solution/gel transition; CS 80/100 and β-GP solution remained stable for some days. CS 95/100 and β-GP solution was very unstable in refrigerated conditions, it remained stable for less than 4 hours. While when using CS 95/100 and G1-P, results were better. CS 95/100 and G1-P solution remained stable for some days in refrigerated conditions.

A DD of 80/100 guaranteed more stability of the solution in such conditions. On the other hand, when using G1-P the stability of the solution was higher too.

Between the best 3 candidates for bioprinting, CS 95/100 2% w/v R=4.5 with DMEM and G1-P solution was the one that was more stable in refrigerated conditions.

In this study, it was observed that gelation time was influenced by the concentration of gelling agent added to the final solution; it was controlled by R, so increasing R which means adding more grams of salt, a faster gelation time was achieved. It can be explained by means of pH values; increasing the

gelling agent concentration leads to an increase in pH which in turn induces a reduction of CS protonation and intermolecular electrostatic repulsion, thereby promoting the solution/gel transition, as Supper *et al.,* showed in 2013 [9].

Supper *et al.,* [9] studied the properties of CS/β-GP solutions by varying some parameters. They mentioned that a reduction in gelation time was achieved by increasing the final polymer concentration in the solution. In the same study, Supper et al., [9] also mentioned that a sharp increase in CS concentration leads to a highly viscous solution, hindering the diffusion of CS and salt and slowing down the gelation process.

On the contrary, in other study, *Supper et al.,* [11] studied the properties of CS/G1-P solutions. They mentioned that decreasing the concentration of CS in the final solution gave rise to a decrease in the gelation time. Thus, demonstrating that CS/β-GP and CS/G1-P have an opposite behaviour when the final polymer concentration is varied.

In this study, solutions of CS 95/100 and G1-P acted as Supper et al., demonstrated in 2014 [11]; a reduction in gelation time was achieved by decreasing the final polymer concentration. However, it was observed that a further decrease of CS concentration did not further accelerate the gelation, as it was observed in CS 95/100 1.75% w/v R equal to 4.5 and G1-P solution.

Comparing results from table 2 and table 3, it was noted that gelling agent affected gelation time. When using G1-P, the gelation time was approximately four times higher than when using β-GP at same concentrations. An example using CS 80/100 is showed in table 6.

Final solution concentration (% w/v)	**R**	**Gelling agent solvent**	**T_{gel} β-GP (min)**	**T_{gel} G1-P (min)**
1.5	5	Ultrapure water	20	90
1.5	7	Ultrapure water	15	60

Table 6. Comparison of gelation times using β-GP and G1-P.

The solvent in which the salt was dissolved also affected the gelation time. DMEM accelerated the solution/gel transition in comparison to ultrapure water. An example using CS 80/100 (4.5% w/v, HCl 0.2M) and β-GP is showed in table 7.

Final solution concentration (% w/v)	R	Gelling agent solvent	T_{gel} β-GP (min)
1.5	8	Ultrapure water	13
1.5	8	DMEM	5

Table 7. Comparison of gelation times using ultrapure water and DMEM.

Almost all solutions displayed a pH in the physiological range, which was of great importance because the hydrogel was designed to incorporate cells. Those solutions that showed a pH higher than 7.4 [13], the limit of the physiological range, reduced the pH when DMEM was used to solve the gelling agent instead of ultrapure water.

4.2. pH measurements during gelation process

The pH of two different solutions was monitored while gelation process was taking place. These solutions were CS 95/100 2.5% w/v R=4 with DMEM and β-GP, and CS 95/100 2% w/v R=4.5 with DMEM and G1-P, two of the best candidates for bioprinting.

The pH showed a clear decrease along hydrogel formation and once gelation was achieved, the pH remained stable, as it is observed in figure 15.

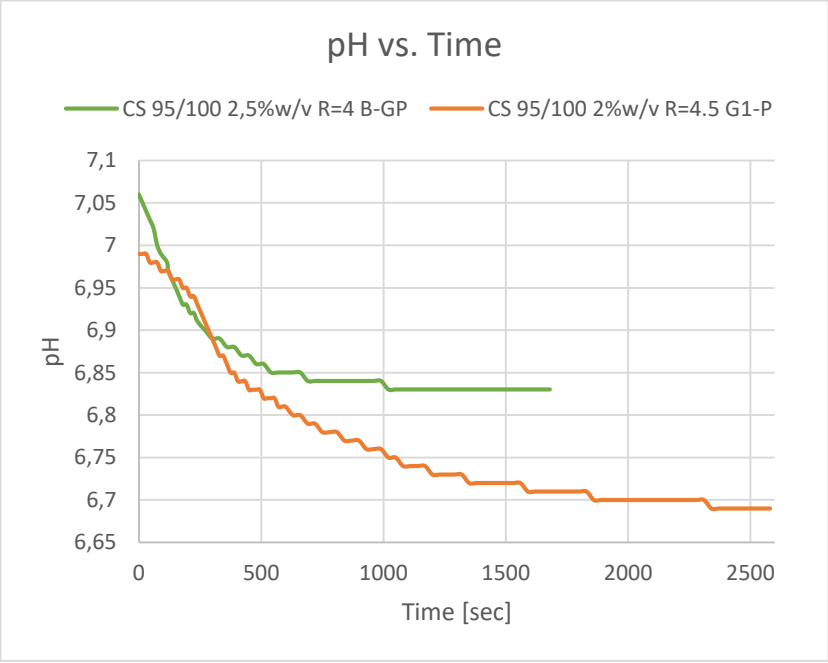

Figure 15. pH as a function of time during gelation process of CS 95/100 2,5% R=4 β-GP solution and CS 95/100 2% R=4.5 G1-P solution.

Supper *et al.,* [8] observed the same behaviour in their studies in 2014. They considered the gelation point as the point in which the pH remains stable.

For CS 95/100 2.5% w/v R=4 with DMEM and β-GP, there was a reduction of the pH from 7.06 to 6.83 once hydrogel was formed. The point at which the pH was considered stable was ~750 sec.

For CS 95/100 2% w/v R=4.5 with DMEM and G1-P, there was a reduction of the pH from 6.99 to 6.69 once hydrogel was formed. The point at which the pH was considered stable was ~1710 sec.

Gelation times of these solutions (paragraph 4.1.) showed that the solution that contained G1-P had a slower solution/gel transition process. The same behaviour is observed regarding the pH of both solutions, as CS 95/100 2% w/v R=4.5 with DMEM and G1-P solution took more time in achieving a stable pH.

4.3. Degradation test

The degradation test allowed to characterize the ability of the hydrogel to absorb water, the weight loss of the hydrogel and the behaviour of the pH in physiological conditions, ~37°C and PBS.

Before presenting the results, it is important to mention that CS 80/100 1.5% w/v R=8 with DMEM and β-GP hydrogel was discarded after one day in contact with PBS solution because the hydrogel was dissolved in PBS solution and there was no phase separation between hydrogel and PBS, so when PBS was tried to be removed, rests of hydrogel were removed too. The hydrogel was completely degraded.

So, results and discussion of degradation test of the other two hydrogels, CS 95/100 2% w/v R=4.5 with DMEM and G1-P hydrogel, and CS 95/100 2.5% w/v R=4 with DMEM and β-GP hydrogel, are presented. In order to differentiate them, results are expressed as CS/G1-P when it is referred to the first solution, and CS/β-GP when it is referred to the second solution.

The Equilibrium Water Content (EWC %) was monitored after 1 hour, 1 day, 4 days, 7 days and 14 days. In figure 16, it can be observed that CS/PP hydrogels were able to increment the content of water when they were in contact with PBS solution.

CS/G1-P hydrogel was able to increment its water content from ~85% to 91% in one day and then the water content remained stable until 14 days of study. While CS/β-GP hydrogel was able to increment its water content from ~88% to 93% and then the water content remained also stable. The increment of water using different gelling agent is nearly the same once they are in physiological conditions.

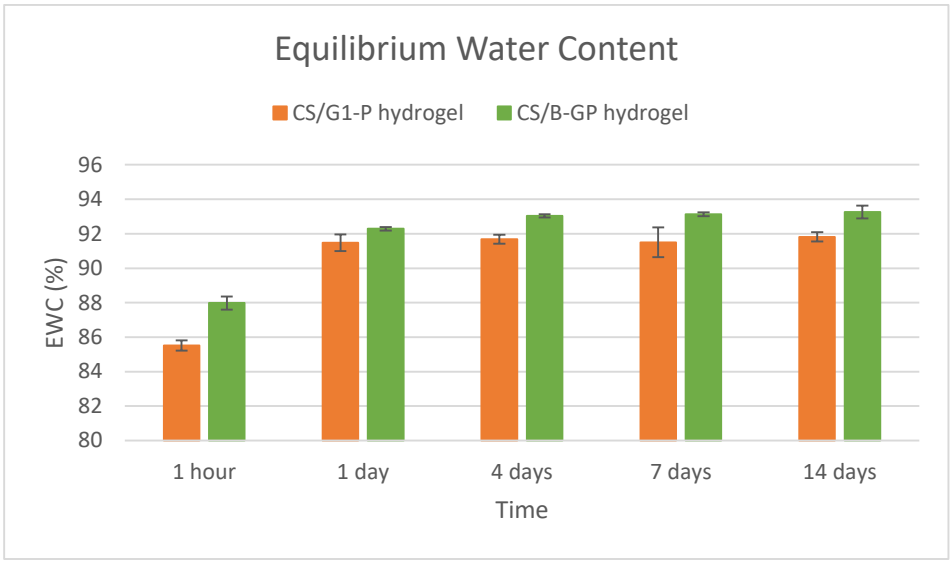

Figure 16. Equilibrium Water Content (EWC %) of CS/G1-P and CS/β-GP hydrogels as a function of the incubation time in PBS at 37°C. Mean of experimental values and SD (n=3) are reported.

The Weight Loss (WL %) was monitored after 1 hour, 1 day, 4 days, 7 days and 14 days. In figure 17, it can be observed that weight loss after one hour in contact with PBS reached a value of ~30% for both hydrogels, then a further increase to ~60% in the weight loss was observed and this value remained stable until 14 days of study. The difference between values using different gelling agents is nearly depreciable, the degradation is very similar.

Figure 17. Weight Loss (WL %) of CS/G1-P and CS/β-GP hydrogels as a function of the incubation time in PBS at 37°C. Mean of experimental values and SD (n=3) are reported.

The observed weight loss can be attributed to a liberation of gelling agent, G1-P and β-GP, into the sample. For CS/G1-P hydrogel, the number of mol of G1-P are 4.5 times the number of mol of amino groups present in CS, while for CS/β-GP the number of mol of β-GP are 4 times the number of mol of

amino groups present in CS, according to equation 3.1. Although gelling agents acted as ionic cross-linking agents in the hydrogel formation, it can be assumed that a major quantity was not involved in any linkage in the solution/gel transition at 37°C. For that reason, it can be supposed that part of gelling agent that was not involved in the process was transferred to PBS solution due to concentration gradient between the hydrogel and PBS solution.

The pH of the PBS solution that was in contact with the CS/G1-P hydrogel decreased from 7.4 to 6.42 in the first 7 days of experiment, then, an increment to 6.56 was achieved during another 7 days. While the pH of the PBS solution that was in contact with the CS/β-GP hydrogel decreased from 7.4 to 6.64 in the first 24 hours of experiment, then, an increment to 6.78 was achieved until the end of the experiment in 14 days.

The decrease of the pH could be attributed to an increase of H_3O^+ ions in the PBS solution. These ions could proceed from the diffused salt (β-GP or G1-P) that had incorporated the ions from the protonated amino groups present in the CS/PP solution with an increase of temperature.

Then, the increase of pH could be attributed to a decrease of H_3O^+ ions that bind to the amino groups that have been released with the degradation of CS.

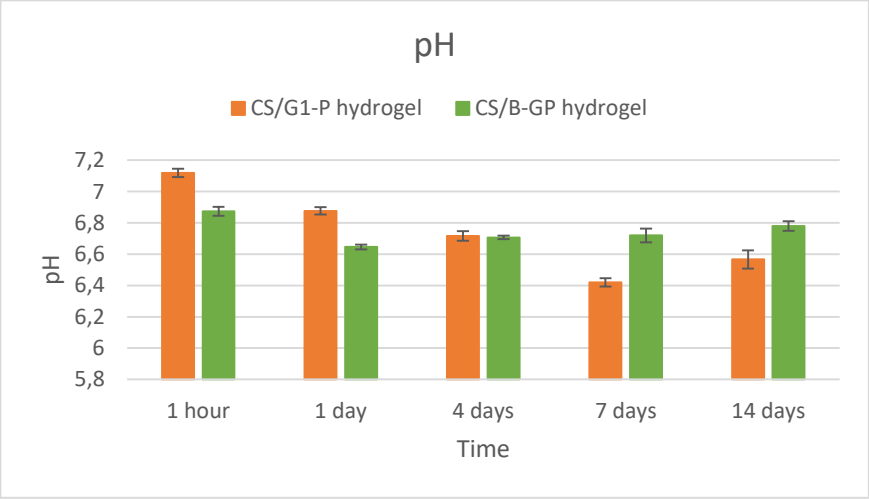

Figure 18. pH of CS/G1-P and CS/β-GP hydrogels as a function of the incubation time in PBS at 37°C. Mean of experimental values and SD (n=3) are reported.

4.4. Degradation test with lysosome

In this paragraph, results and discussion of the degradation test performed adding lysosome to PBS solution are shown. Results are expressed as a comparison between both degradation tests, the one without lysosome and the other with lysosome is shown to have a better comprehension of them and to see the difference.

Two hydrogels were tested, CS 95/100 2% w/v R=4.5 with DMEM and G1-P hydrogel, and CS 95/100 2.5% w/v R=4 with DMEM and β-GP hydrogel. In order to differentiate them, results are expressed as CS/G1-P when it is referred to the first solution, and CS/β-GP when it is referred to the second solution.

The Equilibrium Water Content (EWC %) showed that of CS/G1-P hydrogel was able to swell more water when lysosome was present in PBS solution. The difference of this increment was about less than 10% in the first hour and then less than 2% in the following days.

In the case of CS/β-GP hydrogel, it was able to swell ~6% of water more than when no lysosome was added, but then, the increment of water was quite similar using or not lysosome.

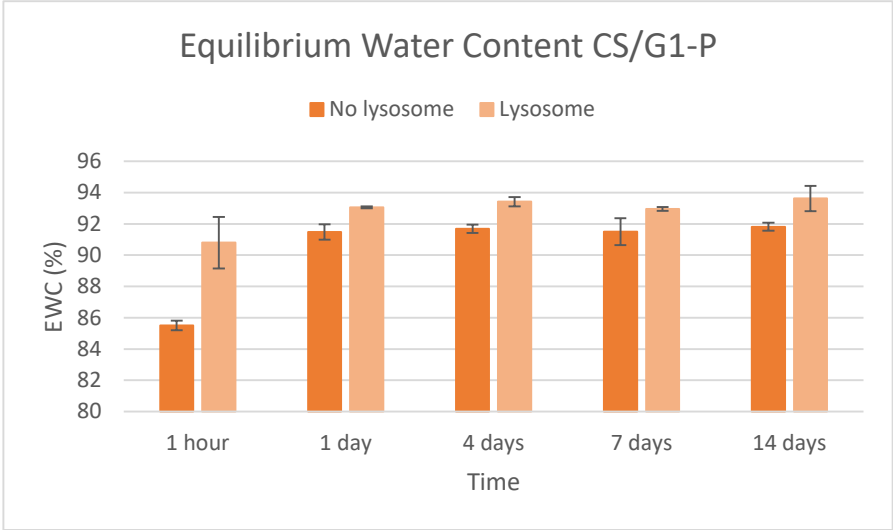

Figure 19. Equilibrium Water Content (EWC %) of CS/G1-P hydrogel when no addition and addition of lysosome to PBS solution, as a function of the incubation time in PBS at 37°C. Mean of experimental values and SD (n=3) are reported.

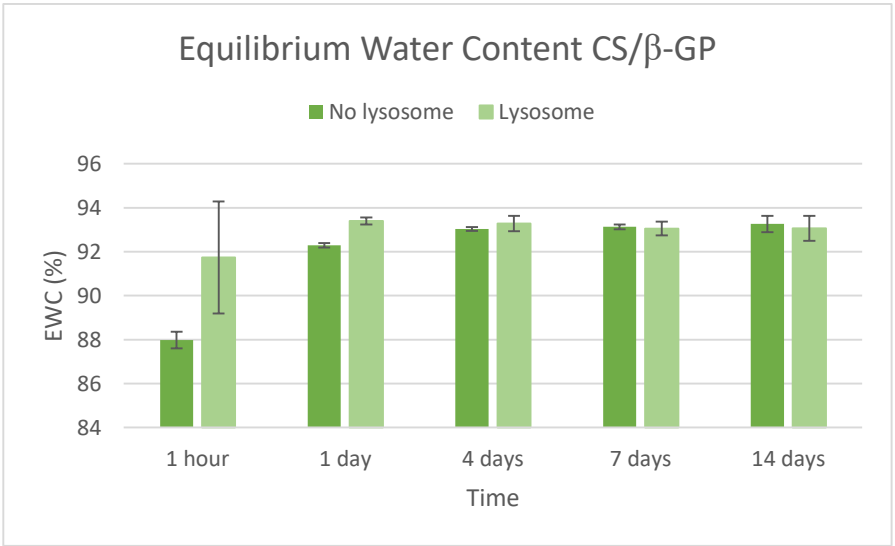

Figure 20. Equilibrium Water Content (EWC %) of CS/β-GP hydrogel when no addition and addition of lysosome to PBS solution, as a function of the incubation time in PBS at 37°C. Mean of experimental values and SD (n=3) are reported.

On the one hand, for CS/G1-P hydrogel, the weight loss that the hydrogel suffered due to its degradation was higher in comparison to when no lysosome was added to PBS solution. This was the effect of lysosome, characterized by the degradation of CS. However, the difference of this increment was more pronounced in the first hour of experiment, about ~20% higher, and then ~5-10%.

On the other hand, for CS/β-GP hydrogel, the weight loss was ~20% higher in the first hour of experiment in comparison to when no lysosome was added to PBS solution. Then, during the first four days of experiment values of weight loss continued to be ~5% higher, while after seven days of experiment values of weight loss were ~3% lower in comparison to when no lysosome was added to PBS solution.

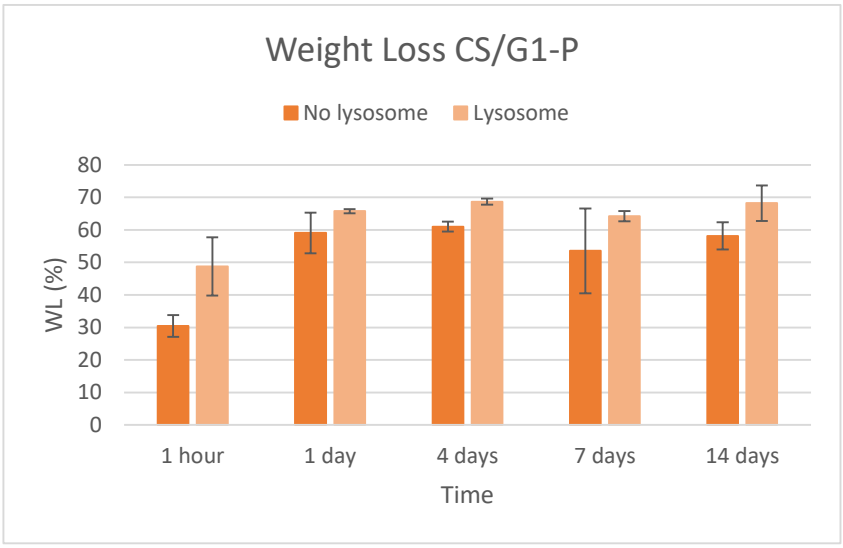

Figure 21. Weight Loss (WL %) of CS/G1-P hydrogel when no addition and addition of lysosome to PBS solution, as a function of the incubation time in PBS at 37°C. Mean of experimental values and SD (n=3) are reported.

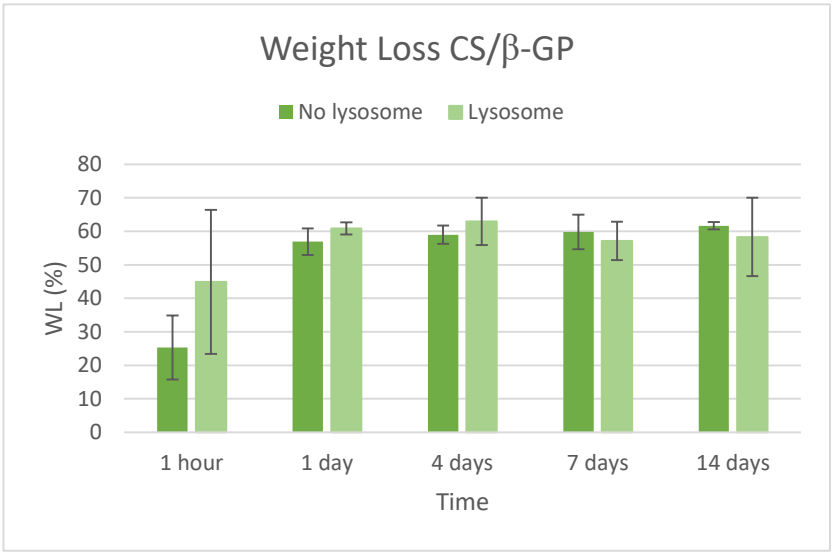

Figure 22. Weight Loss (WL %) of CS/β-GP hydrogel when no addition and addition of lysosome to PBS solution, as a function of the incubation time in PBS at 37°C. Mean of experimental values and SD (n=3) are reported.

Differences on weight loss adding or not lysosome to PBS solutions were not very remarkable. This can be attributed to the concentration of lysosome that was added, 1 mg/mL, the one found in literature. If the concentration had been greater, the effect on degradation could have been more remarkable.

Major differences were found in the behaviour of pH. When lysosome was added to PBS solution, the decrease of pH was more gradual and less variable than when no lysosome was added. This behaviour was observed in both hydrogels.

This gradual decrease of pH could be attributed to two factors:

- First, a decrease of the pH caused by an increase of H_3O^+ ions in the PBS solution. These ions could proceed from the diffused salt (β-GP or G1-P) that had incorporated the ions from the protonated amino groups present in the CS/PP solution with an increase of temperature.
- Then, an increase of pH caused by a decrease of H_3O^+ ions that bind to the amino groups that have been released with the degradation of CS.

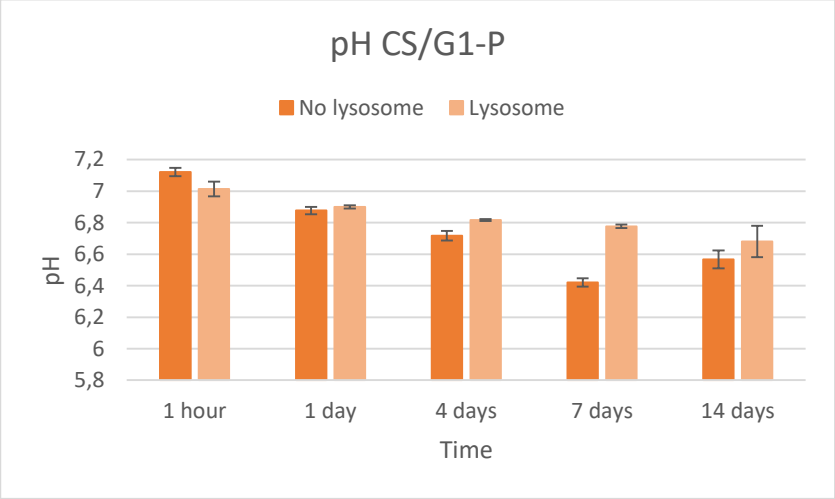

Figure 23. pH of CS/G1-P hydrogel when no addition and addition of lysosome to PBS solution, as a function of the incubation time in PBS at 37°C. Mean of experimental values and SD (n=3) are reported.

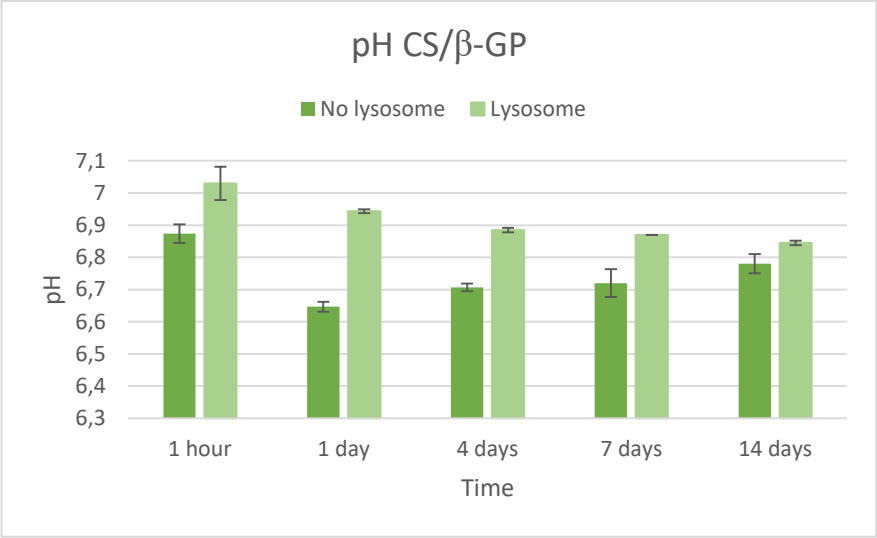

Figure 24. pH of CS/β-GP hydrogel when no addition and addition of lysosome to PBS solution, as a function of the incubation time in PBS at 37°C. Mean of experimental values and SD (n=3) are reported.

4.5. Kaiser test

Results of absorbance are shown in this section. These values indicate the amount of free amino groups liberated by the CS after its degradation in PBS plus lysosome solution of two hydrogels, CS 95/100 2% w/v R=4.5 with DMEM and G1-P hydrogel referred as CS/G1-P hydrogel, and CS 95/100 2.5% w/v R=4 with DMEM and β-GP hydrogel referred as CS/β-GP hydrogel.

As higher the values, higher was the presence of free amino groups. The degradation of both hydrogels was similar in terms of liberated amino groups. Values of absorbance were almost the same for both hydrogels; this means that close amounts of free amino groups were liberated.

Some differences between values, as the ones coloured in orange that showed high values, or the ones coloured in nearly blue that showed low values, can be attributed to experimental errors committed during the test. Values like 0.035, 0.036 and 0.037 were low because these positions in the microplate were empty, there was no sample to read.

	CS/G1-P hydrogel			Average
1 hour	1,222	0,929	0,550	0,900
1 day	0,462	0,396	0,036	0,429
4 days	0,786	0,645	0,706	0,712
7 days	0,703	0,435	0,508	0,549
14 days	0,824	0,587	1,065	0,825

	CS/β-GP hydrogel			Average
1 hour	0,383	0,766	0,747	0,632
1 day	0,610	0,768	0,496	0,625
4 days	0,037	0,897	0,738	0,557
7 days	0,807	0,644	0,666	0,706
14 days	0,714	0,665	0,035	0,690

Table 8. Absorbance of samples to detect the presence of free amino groups; as higher the value, higher the presence of free amino groups. Values coloured in blue were not taken into account to calculate the average.

4.6. Rheological measurements

In the following section, results and discussion of rheological measurements of two different solutions, CS 95/100 2% w/v R=4.5 with DMEM and G1-P, and CS 95/100 2.5% w/v R=4 with DMEM and β-GP solution, are shown. In order to differentiate them, results are expressed as CS/G1-P when it is referred to the first solution, and CS/β-GP when it is referred to the second solution.

Shear Strain Test

Values of Storage Modulus (G') and Loss Modulus (G'') for different values of strain are shown in figure 25.

For the two different solutions, CS/G1-P and CS/β-GP, values of shear strain at which G' and G'' are linear and parallel were similar. These values of shear strain went from 0.1 to 10 % approximately. Finally, a value of shear strain of 1% was selected to perform the other rheological measurements.

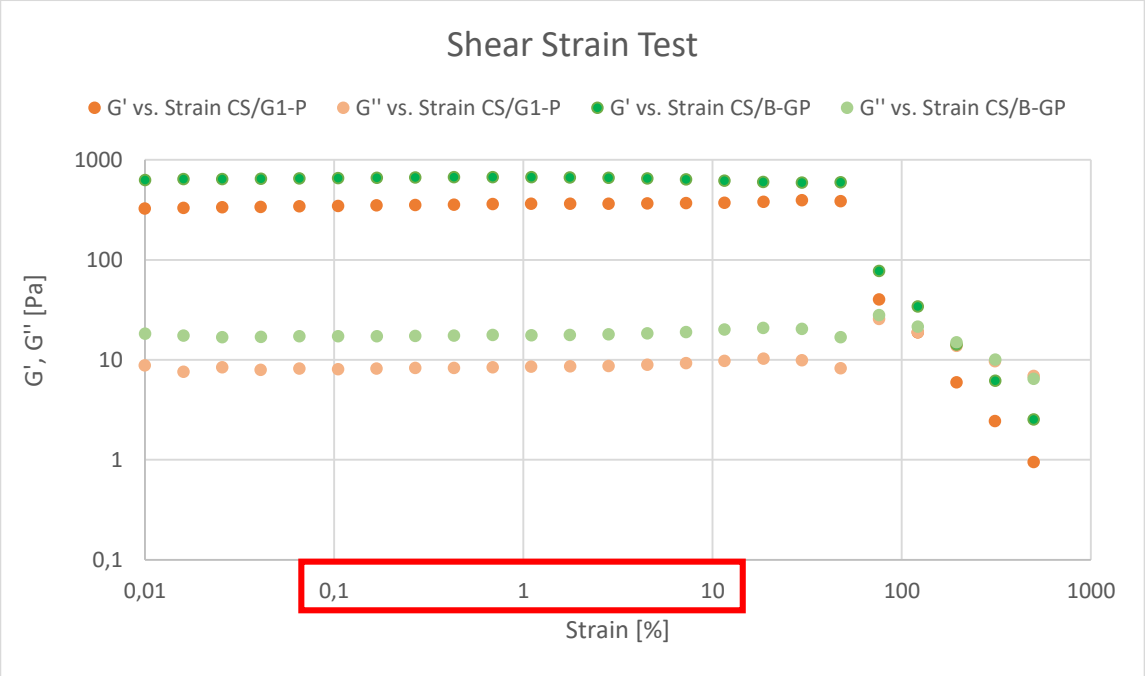

Figure 25. Storage Modulus (G') and Loss Modulus (G'') as a function of shear strain of CS 95/100 2,5% R=4 β-GP solution and CS 95/100 2% R=4.5 G1-P solution.

Ramp Sweep Test

Different values of viscosity were observed in response to an increase on temperature at constant continuous rotation in figure 26. This test was done at different rates of increase of temperature, at 0.5°C/min, 1°C/min, 1.5°C/min and 2°C/min, but rate of 1.5°C/min was considered as the best rate.

Two points are of major interest in figure 26, the point that belongs to the onset temperature (red), it is the temperature at which the solution/hydrogel transition starts, and the point that belongs to the maximum viscosity temperature (blue). It was observed that the solution/hydrogel transition for CS/β-GP started before than the solution/hydrogel transition for CS/G1-P, at a temperature of ~27°C while the second one started at ~35°C.

It was also observed that viscosities of CS/β-GP solution were higher than viscosities of CS/G1-P solution, they varied in approximately one order of magnitude once gelation was achieved. When the hydrogel was formed, the maximum viscosity of CS/ β-GP solution was ~340 Pa·s, while the maximum viscosity of CS/G1-P was 17 Pa·s. Among the big difference of viscosities, viscosities ranging from 30 mPa/s to $6 \cdot 10^7$ mPa/s are characteristic for hydrogels [5].

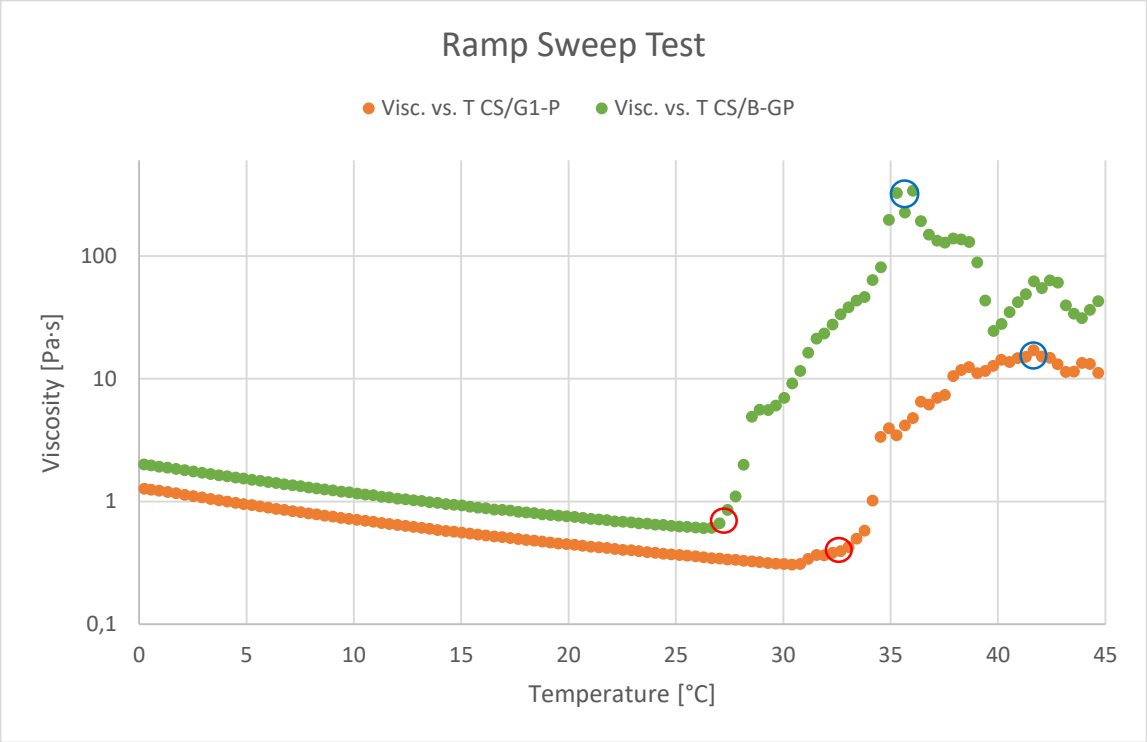

Figure 26. Viscosity of CS 95/100 2,5% R=4 β-GP solution and CS 95/100 2% R=4.5 G1-P solution at different temperatures.

Time Sweep Test

Values of Storage Modulus (G') and Loss Modulus (G'') depending on time at constant rotational oscillation and temperature are shown in the following figures. When G' and G'' cross, it means, G' becomes higher than G'', the value of time belonging to this point is the exact time at which the solution becomes a hydrogel [8]. Increasing the time at 37°C the strength of the hydrogel increased to reach a maximum value after ~20 minutes.

Three different samples of CS/G1-P solution were studied and the gelation times were $t_{S/G}$=252 s, $t_{S/G}$=252 s and $t_{S/G}$=240 s. Thus, a gelation time of $t_{S/G}$=248 s was considered as the correct value.

CS/G1-P solution with a concentration of CS 95/100 of 2% w/v and R=4.5 became a hydrogel after 4 min and 8 secs.

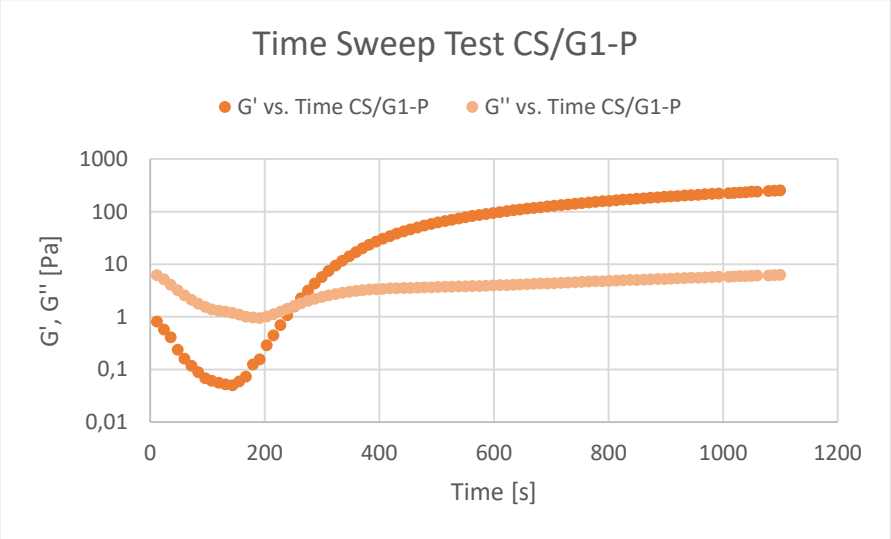

Figure 27. Representative plot of Storage Modulus (G') and Loss Modulus (G'') as a function of time of CS 95/100 2% R=4.5 G1-P solution.

Two samples of CS/β-GP solution were studied and the gelation times were $t_{S/G}$=156 s and $t_{S/G}$=132 s. Thus, a gelation time of $t_{S/G}$=144 s was considered as the correct value.

CS/β-GP solution with a concentration of CS 95/100 of 2.5% w/v and R=4 became a hydrogel after 2 min and 24 secs.

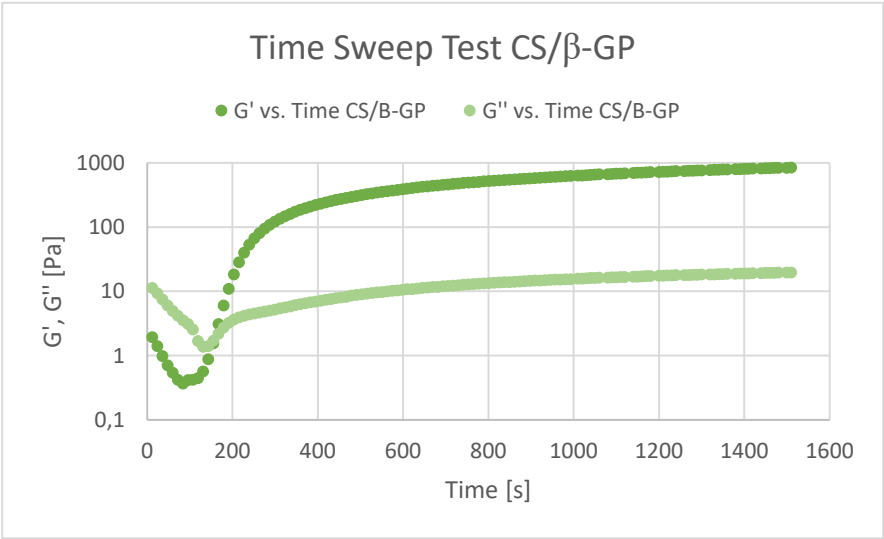

Figure 28. Representative plot of Storage Modulus (G') and Loss Modulus (G'') as a function of time of CS 95/100 2,5% R=4 β-GP solution.

Thus, comparing both CS/PP solutions, it can be said that CS/β-GP solution displayed a reduction of approximately the half of gelation time in comparison with CS/G1-P solution, confirming the impact of the nature of the gelling agents on the gelation times. These results match with the ones reported in paragraph 4.1., the gelation time is doubled when G1-P instead of β-GP is used.

If values of G' and G'' are compared, it is noticeable that values for CS/β-GP solution are higher. CS/PP solutions with G' values comprised between 1 and 10 KPa and with G'>>G'' display a strong gel behaviour [8]. Values of G' are ~1000 Pa and, > 10 Pa for G'' for CS/β-GP solutions. While values of G' are ~100 Pa and between 1 and 10 Pa for G'' for CS/G1-P solution. Thus, these values proved that the CS/β-GP hydrogel was stronger than the CS/G1-P hydrogel.

Three samples of CS/G1-P solution were studied to see the behaviour of the gelation time after 10 and 14 days of storage in the fridge. Some changes can be observed in the figure 29.

After 14 days, the gelation time was $t_{S/G}$=36.5 s, and after 10 days the gelation time was $t_{S/G}$=180 s. The reduction in time was significant, but it is important to mention that the appearance of both solutions was different between them. The solution that was stored for 14 days was more viscous by visual inspection. This difference was also appreciated in the values of G' and G'', that were higher for the solution of 14 days. CS/PP solutions with G' values comprised between 1 and 10 KPa and with G'>>G'' display a strong gel behaviour [8]. Thus, it can be said that the solution stored for 14 days was stronger than the one that was stored for 10 days once they are a hydrogel.

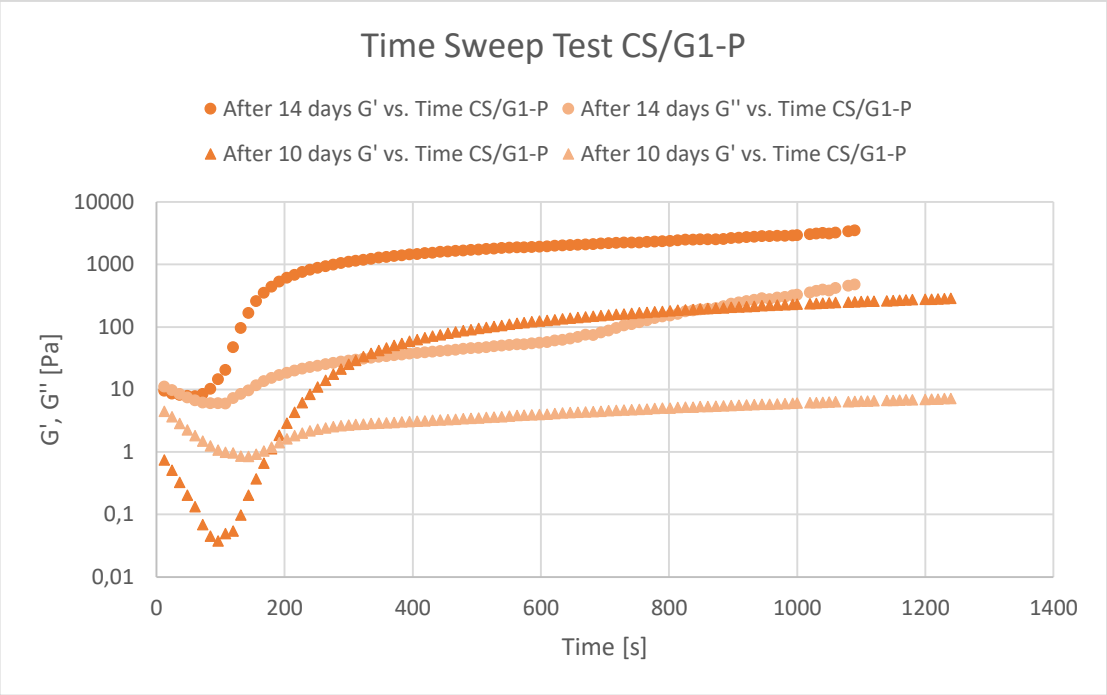

Figure 29. Storage Modulus (G') and Loss Modulus (G'') as a function of time of CS 95/100 2% R=4.5 G1-P solution after 14 and 10 days of storage.

Temperature Sweep Test

Values of Storage Modulus (G') and Loss Modulus (G'') depending on temperature at constant rotational oscillation are shown in the following figures. The progression of G' and G" showed a clear sol/gel transition for each CS/PP system, when G' becomes higher than G". The value of temperature belonging to this point is the exact temperature at which the solution becomes a hydrogel [8].

Two different samples of CS/G1-P solution were studied and the gelation temperatures were $T_{S/G}$=35.79°C and $T_{S/G}$=36.5°C.

Thus, a transition temperature of $T_{S/G}$=36.15°C was considered as the correct value for CS/G1-P solution. This result was similar to the one achieved in Ramp Sweep Test, that was 35°C.

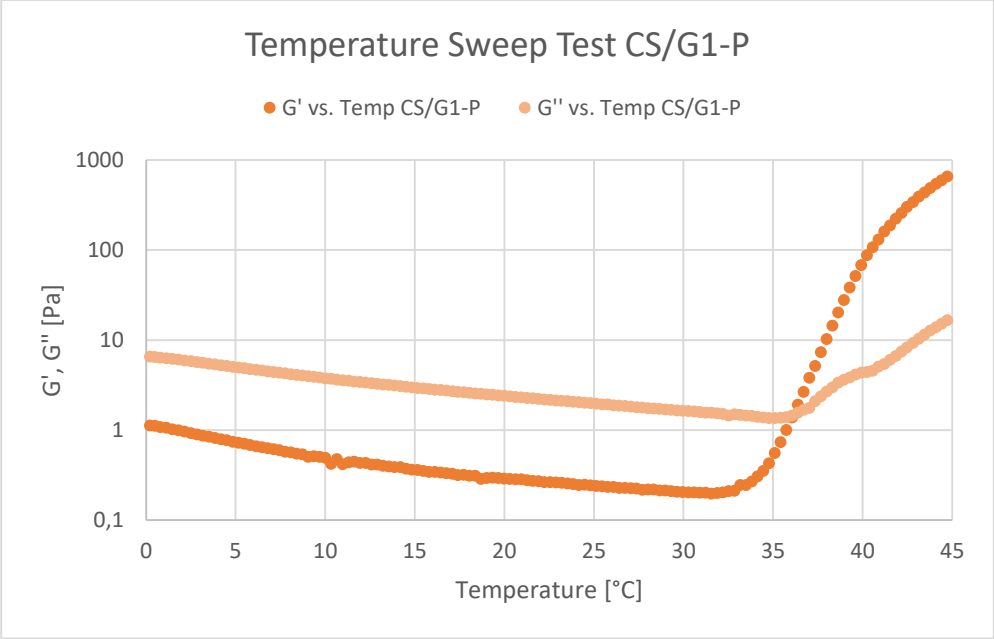

Figure 30. Representative plot of Storage Modulus (G') and Loss Modulus (G'') as a function of temperature of CS 95/100 2% R=4.5 G1-P solution.

Two samples of CS/β-GP solution were studied and the gelation temperatures were $T_{S/G}$=32.22°C and $T_{S/G}$=27.57°C.

Thus, a transition temperature of $T_{S/G}$=29.9°C was considered as the correct value for CS/β-GP solution. This result was similar to the one achieved in Ramp Sweep Test, that was 27°C.

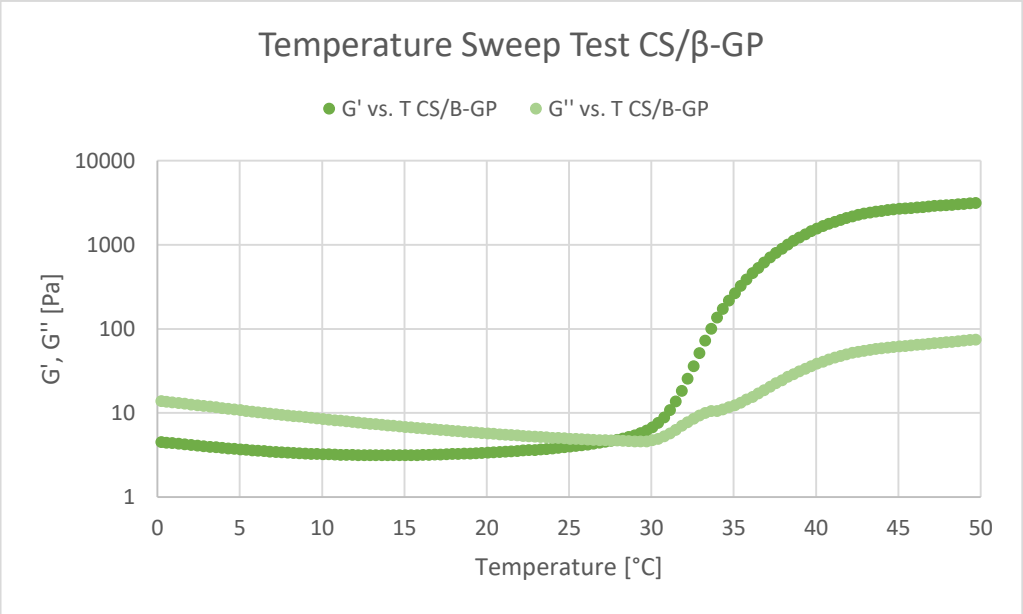

Figure 31. Representative plot of Storage Modulus (G') and Loss Modulus (G'') as a function of temperature of CS 95/100 2,5% R=4 β-GP solution.

Comparing both transition temperatures, it was observed that less temperature was required to obtain a hydrogel if gelling agent β-GP was present in the solution. This result confirmed the clear influence in the chemical structure of the gelling agents on the gelation temperature.

Thixotropy test

CS/PP solutions were tested for the thixotropy test.

In this test, three different phases were observed. In the first phase of rotational oscillation, the difference between G' and G'', being G'>>G'', confirmed the hydrogel structure.

In the second phase of continuous rotation, values of viscosity decreased when shear rate was applied, breaking the internal network structure of the hydrogel.

At the beginning of the third phase of rotational oscillation, it was observed that G'' was bigger than G' and immediately a crossover between both, rising G'. This behaviour is characteristic of the solution/gel transition. The last part showed how the hydrogel recovered its viscosity; after ceasing the shear rate, the hydrogel rebuilt its internal network structure. It is observed when G' is bigger than G'' and they are parallel [8].

The hardness of the hydrogel was recovered once shear rate was ceased because G'>G'', but this hardness was different from the one that it was observed at the beginning of the test. This is known because values of G' and G'' were lower at the end.

Differences between G1-P and β-GP were observed performing this test. In the first phase, values of G' and G'' were higher when β-GP was used, and also the separation between both values was higher, proving that CS/β-GP hydrogel is stronger than CS/G1-P hydrogel because G'>>G''.

In the second phase, values of viscosity decreased more for G1-P from 106 to 12 Pa·s, while values of viscosity of β-GP decreased from 140 to 86 Pa·s. Thus, CS/β-GP hydrogel is more viscous than CS/G1-P hydrogel and maintained better the viscosity when the internal network structure of the hydrogel was broken.

In the last phase of the test, CS/G1-P hydrogel recovered its hardness but the final hydrogel was softer than the one from the beginning because values of G' and G'', and the separation between both were lower. On the contrary, CS/β-GP hydrogel recovered better its initial structure because values of G' and G'' at the end of the test were pretty much similar to those from the beginning of the test.

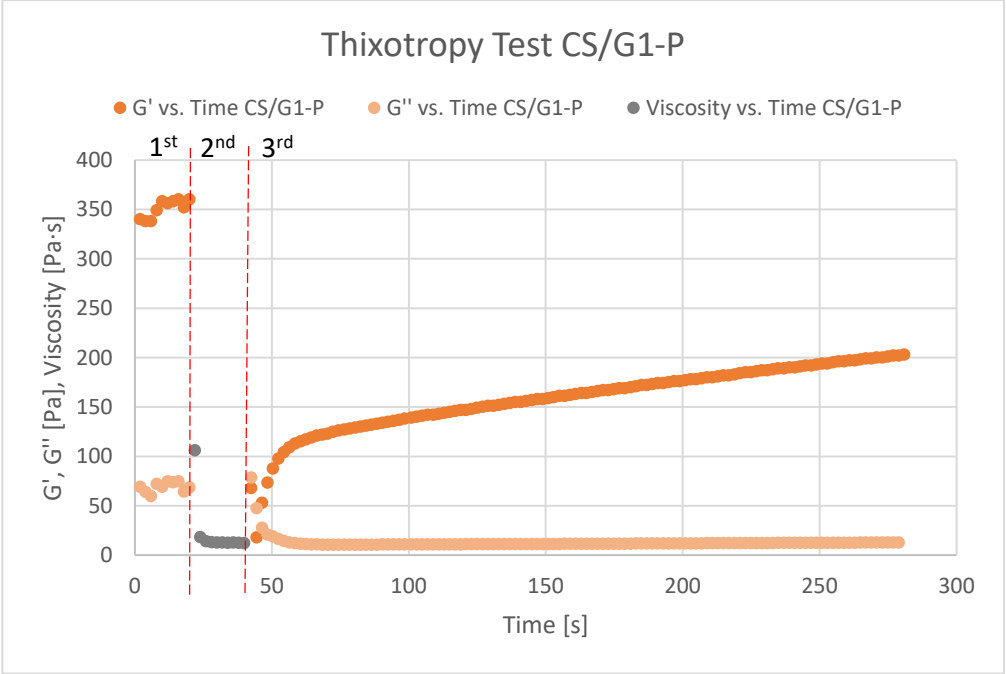

Figure 32. Storage Modulus (G'), Loss Modulus (G'') and Viscosity as a function of time of CS 95/100 2% R=4.5 G1-P solution.

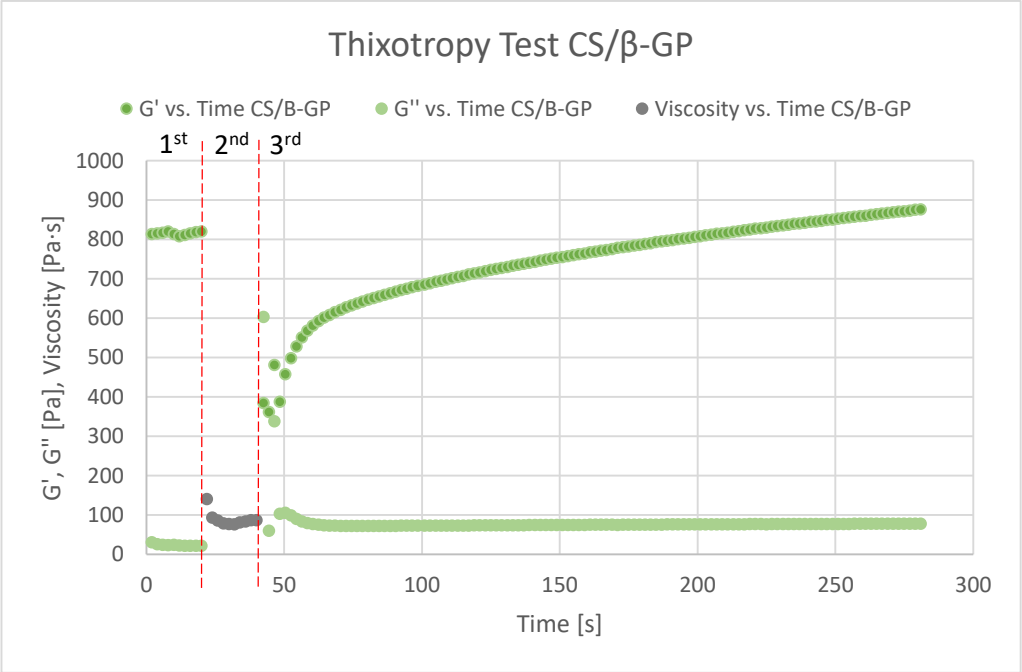

Figure 33. Storage Modulus (G'), Loss Modulus (G'') and Viscosity as a function of time of CS 95/100 2,5% R=4 β-GP solution.

Viscosity vs. Shear Rate

Different values of viscosity were observed in response to an increase on shear rate. In both hydrogels, the decrease in viscosity is very pronounced as it goes from a viscosity from ~300 Pa·s to ~0.5 Pa·s for CS/G1-P, and from ~1250 Pa·s to ~0.5 Pa·s for CS/β-GP. The final viscosity was nearly the viscosity of water which is 0.1 Pa·s.

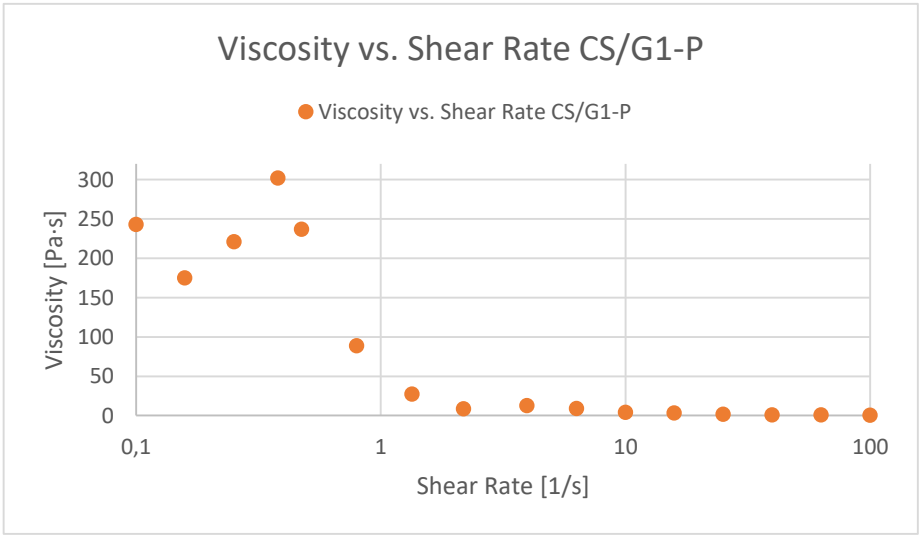

Figure 34. Viscosity as a function of shear rate of CS 95/100 2% R=4.5 G1-P solution.

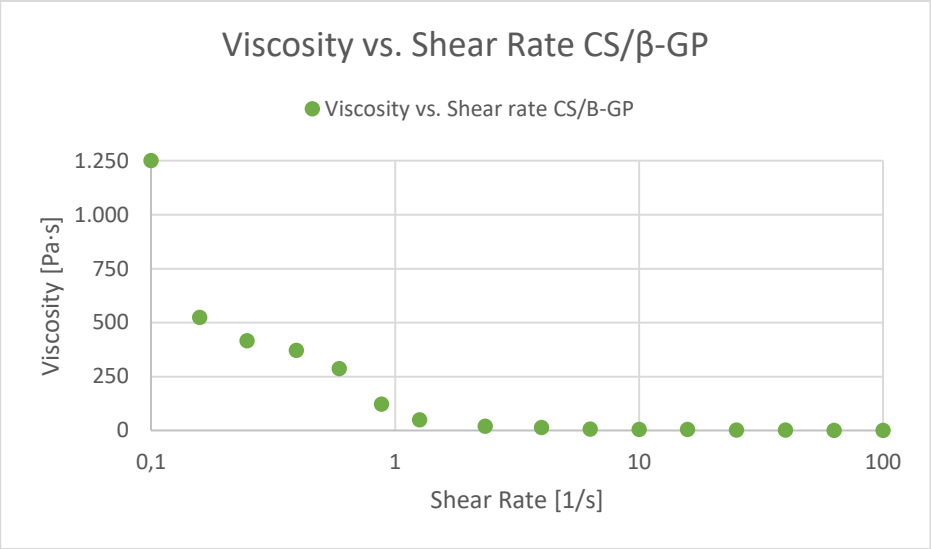

Figure 35. Viscosity as a function of shear rate of CS 95/100 2,5% R=4 β-GP solution.

Results showed in Thixotropy Test and Viscosity vs. Shear Rate Test confirmed that CS/PP hydrogels possessed shear-thinning properties. This non-Newtonian material behaviour causes a decrease in viscosity in response to increases in shear rate.

Materials with shear-thinning properties are commonly used for microextrusion applications. The high shear rates that are present at the nozzle during biofabrication allow these materials to flow through the nozzle, and upon deposition, the shear rate decreases, causing a sharp increase in viscosity [5].

Frequency sweep test

Results showed in figure 36 and figure 37 concern the frequency sweep tests of CS/PP solutions at different temperatures with increasing angular frequency. Values of G' and G'' show the behaviour of the solution at different temperatures of 20°C, 30°C and 37°C.

For higher temperatures as 30° and 37°C, both systems, CS/G1-P and CS/β-GP, displayed gel behaviour as values of G' and G'' exhibit parallel lines and G'>G''. The difference between both temperatures was the strength of the gel, showing a stronger gel at 37°C because values of G' and G'' were higher and the difference between the two values was bigger than for 30°C. These results confirmed the importance of the temperature in the systems to induce gelation.

For lower temperatures as 20°C, both systems, CS/G1-P and CS/β-GP, displayed viscoelastic solid-like behaviour. This behaviour means that at low frequencies G' is bigger than G'' and they are not parallel, indicating that the material behaves as a solid. For some systems with large or heavy particles, the gel structure is not enough to prevent sedimentation of these particles that occurs at low frequencies [16]. The systems of this study could show, in some cases, some particles of CS or gelling agent that were not dissolved in the solution.

Then, for higher frequencies the systems displayed a viscoelastic liquid-like behaviour that is observed when G'' is bigger than G'.

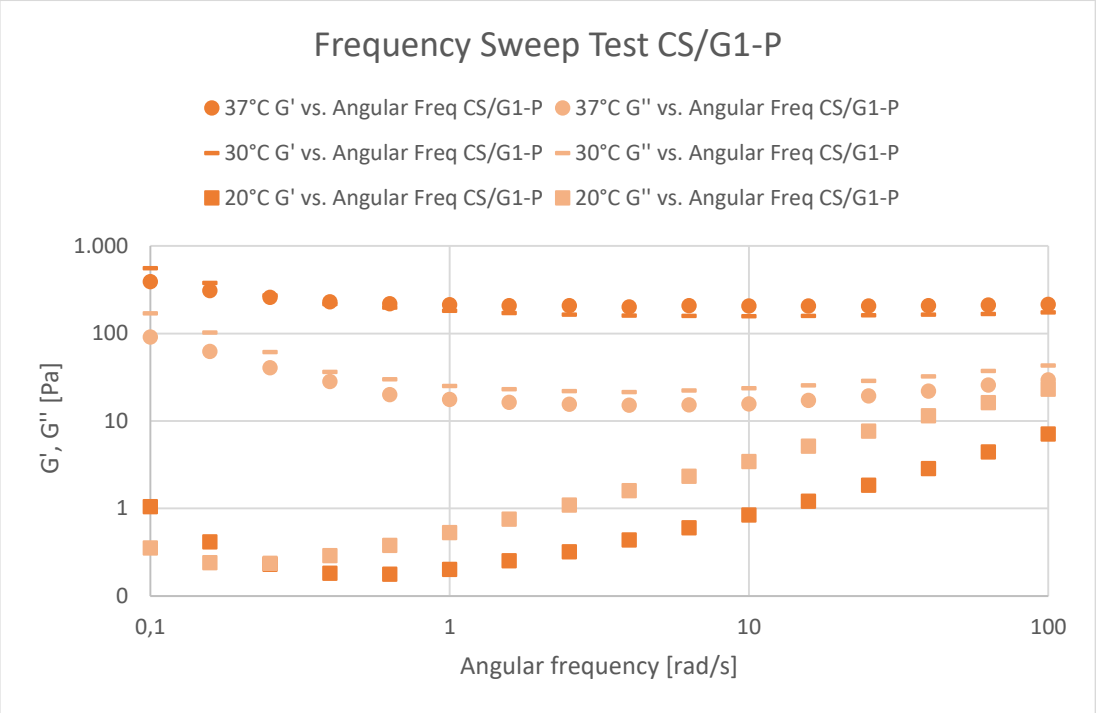

Figure 36. Storage Modulus (G') and Loss Modulus (G'') as a function of angular frequency of CS 95/100 2% R=4.5 G1-P solution.

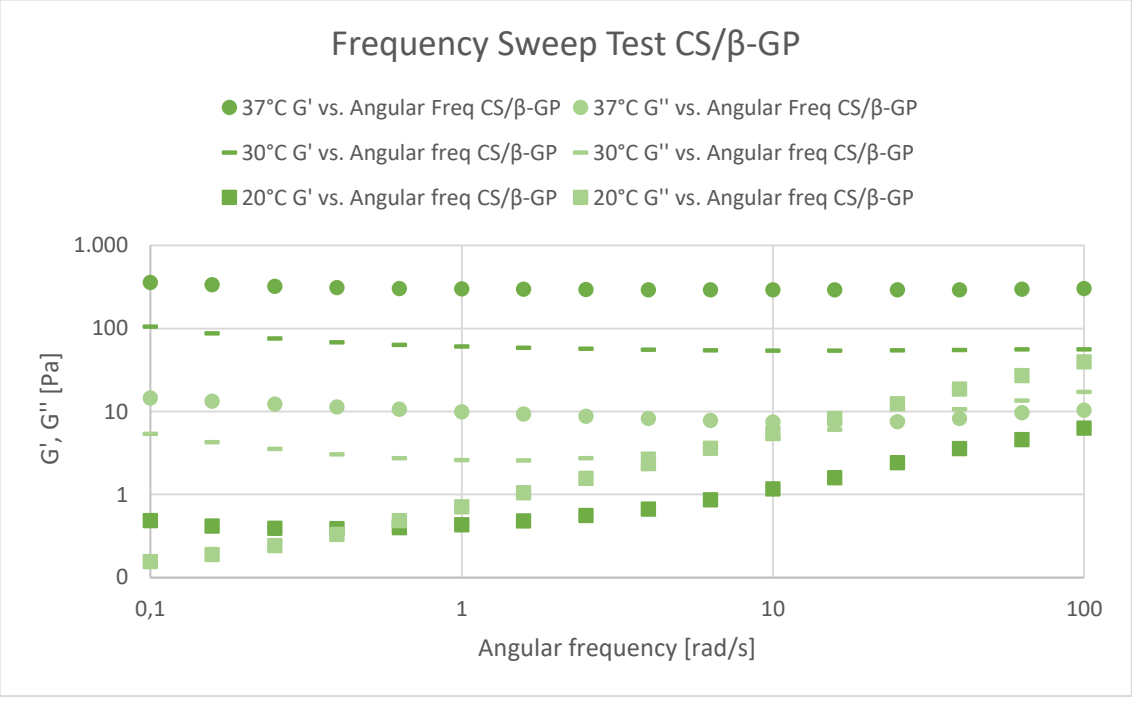

Figure 37. Storage Modulus (G') and Loss Modulus (G'') as a function of angular frequency of CS 95/100 2,5% R=4 β-GP solution.

4.7. Bioprinting

In this paragraph, results on bioprinting of two different solutions are discussed, CS 95/100 2% w/v R=4.5 with DMEM and G1-P, and CS 95/100 2.5% w/v R=4 with DMEM and β-GP solution. In order to differentiate them, results are expressed as CS/G1-P when it is referred to the first solution, and CS/β-GP when it is referred to the second solution.

All possible combinations of parameters mentioned in paragraph 3.5. were tried and some results were better than others.

First of all, PROS and CONS of the parameters are discussed in order to understand why the combinations worked or not:

1. **State of the ink:**
    - Solution form:
        - PROS: extrusion of the ink was achieved easily and pressure was constant during all printing process.
        - CONS: sometimes the gelation was not achieved when the ink touched the surface and all the ink was spread on the surface of the Petri dish or mixed with PBS solution when it was used.
    - Semi-hydrogel form:
        - PROS: no pros were observed.
        - CONS: there were some parts of the semi-hydrogel that were more gelled than others leading to a not uniform semi-hydrogel. This effect caused a constant control and variation on pressure because the not uniform semi-hydrogel had different viscosities and different pressures were needed in order to extrude it. This control on pressure was very difficult to achieve because the pressure was controlled manually, and it was impossible to know when the semi-hydrogel was more gelled. This ink state did not allow the use of all nozzle diameters as it collapsed the tip when small diameters where used.
    - Hydrogel form:
        - PROS: the structure was well maintained when it reached the surface of the Petri dish.
        - CONS: some lumps were present in the hydrogel; the appearance was not homogeneous and it caused the clogging of the nozzle when small diameters were used. This ink state did not allow the use of all nozzle diameters. Another drawback was that high pressures were used to extrude the ink. Before the

ink started flowing, water contained in the hydrogel was expulsed leaving the hydrogel dry due to high pressures that were applied. After water was expulsed, the hydrogel flowed completely dry.

2. **Diameter of the nozzle:**
    - Blue, 22 G:
        - PROS: all states of ink were able to be printed.
        - CONS: no cons were observed.
    - Red, 25 G:
        - PROS: more precise lines were achieved in comparison to blue nozzle.
        - CONS: the tip of the nozzle was sometimes collapsed and the ink did not flow anymore. The tip had to be cleaned or changed constantly.
    - White, 27 G:
        - PROS: more precise lines were achieved in comparison to blue and red nozzle.
        - CONS: the tip of the nozzle was often collapsed and the ink did not flow anymore. The tip had to be changed constantly as the diameter was very small and it could not be precisely cleaned.
3. **PBS solution:**
    - No addition:
        - PROS: rapid adhesion of the ink to the surface of the Petri dish was achieved, avoiding the spreading of the ink.
        - CONS: some parts of the final printed structure were dehydrated and the hydrogel was very dried. There was not a continuous printed structure, there were some gaps where there was no ink.
    - Addition:
        - PROS: the final printed structure was continuous and very hydrated; the aspect was better in comparison to the structure achieved when no PBS was added.
        - CONS: the tip of the nozzle was in contact with PBS at 37°C, this fact sometimes caused a faster gelation in the tip, thus collapsing the nozzle and avoiding the flow of ink.

Table 9 shows in which form the parameters affect to the final printed structure, being in red the worst combinations that gave bad results, in orange the combinations that gave acceptable but improvable results and in green the best combinations that gave the most acceptable results.

	Solution				Semi-hydrogel				Hydrogel			
	CS/G1-P		CS/β-GP		CS/G1-P		CS/β-GP		CS/G1-P		CS/β-GP	
	No PBS	PBS	No PBS	PBS	No PBS	PBS	No PBS	PBS	No PBS	PBS	No PBS	PBS
Blue	4	7	4	7	1	1	1	1	6	2	6	2
Red	4	7	4	5	1	1	1	1	3	3	3	3
White	4	5	4	5	1	1	1	1	3	3	3	3

Table 9. Influence of parameters on the final printed structure. Red: bad. Orange: medium. Green: good.

The red area shows the worst combinations that lead to bad results on bioprinting. Bad results were mainly affected by a combination of the diameter of the nozzle (small diameters) and the state of the ink (semi-hydrogel and hydrogel form). The drawbacks of this area can be divided in three:

1. Ink in semi-hydrogel form was impossible to be printed as explained before in the CONS, so all combinations with semi-hydrogel form were not possible.
2. Spreading of the hydrogel when hydrogel form as state of ink and addition of PBS were combined. The hydrogel was not directly adhered to the surface of the Petri dish and it remained floating due to the presence of PBS solution.
3. Hydrogel form did not allow the printing when small diameters of the nozzle, red and white, were used, causing a clogging in the tip of the nozzle and stopping the flow of the ink.

The orange area shows acceptable combinations but improvable. In this case, drawbacks of these results were affected by the diameter of the nozzle (all diameters had an inconvenient in combination with other parameters), the state of the ink (all states of ink had an inconvenient in combination with other parameters) and the addition or no addition of PBS solution. The most common problems observed in this area can be divided in three:

4. The dryness of some parts of the structure when ink was printed in solution form and PBS was not added. It was mainly affected to the no addition of PBS because PBS solution helped to hydrate the final printed structure.

Figure 38. Dry printed structure.

5. The clogging of the tip of the nozzle leaving the printed structure incomplete, when ink was printed in solution form, the diameters of the nozzle were small and PBS was added, due to the rapid gelation that the solution suffered at the tip of the nozzle in being in constant contact with PBS at 37°C.

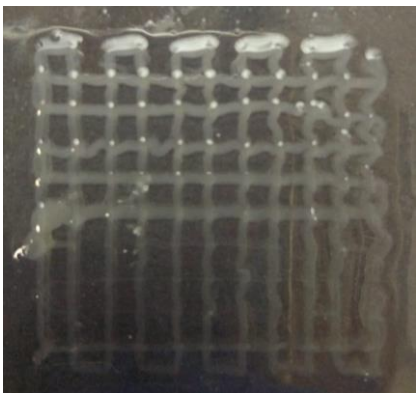

Figure 39. Incomplete printed structure.

6. Non homogeneous hydrogel leaded to a non-uniform final printed structure with the presence of lumps.

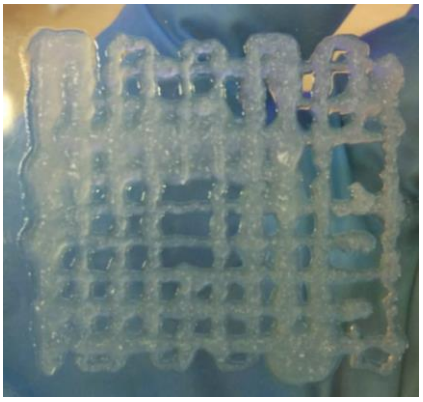

Figure 40. Non homogeneous printed structure.

The green area shows the most acceptable results achieved in bioprinting. Only 3 from 36 possible combinations were considered as the best ones.

7. Very well-defined structures were achieved with solution form, addition of PBS and the use of blue and red nozzles. The key element in this combination was the use of PBS, that speed up the gelation process while hydrated the printed structure.

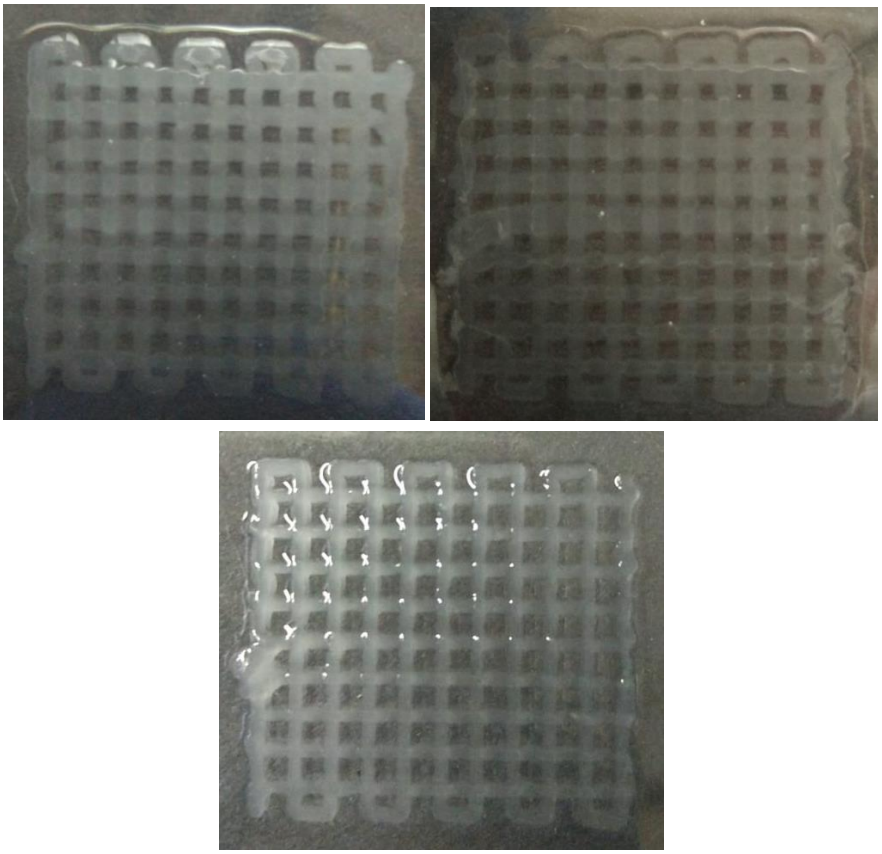

Figure 41. Well-defined printed structures in solution form and PBS addition. Top-left: CS/G1-P with blue nozzle. Top-right: CS/G1-P with red nozzle. Bottom: CS/β-GP with blue nozzle.

No significant differences were observed when CS/G1-P and CS/β-GP solutions were used.

The main difference was that CS/G1-P solution was more homogeneous than CS/β-GP solution; the second one incorporated small precipitates that collapsed the tip of the nozzle, for that reason, small diameters were not useful when this ink was used. The apparition of small precipitates could be attributed to the rapid gelation time and low stability that CS/β-GP solution has.

Results in rheology (see paragraph 4.6.) showed that these two hydrogels have different viscosities, being the CS/β-GP solution more viscous than the CS/G1-P solution. This meant that more pressure was needed when CS/β-GP solution was used. The difference in pressure was low, only 3-4 kPa of difference when using one ink or another.

Another difference between both solutions was the gelation time. Previous results showed that CS/β-GP solution had a faster gelation time than CS/G1-P solution. The effect of gelation time was appreciated in the dryness of the final printed structure. When using CS/β-GP solution without PBS, the structure started to gelify very quickly and when the printer stopped printing the structure was drier in comparison to when using CS/G1-P solution, that had a higher gelation time and the final printed structure took more time in drying.

The effect of gelation time was also appreciated when the structure was printed in solution form and using PBS. When using PBS at 37°C, the tip that contained solution was in contact all the time with PBS. With small diameters of the nozzle, red and white, gelation started at the tip of the nozzle clogging the tip and stopping the flow of the ink. This effect was more pronounced when CS/β-GP solution was used because it had a faster gelation time in comparison to CS/G1-P solution.

Hence, the 3 best combinations of parameters for bioprinting were tested with a more complex structure of 4 layers.

The CS/G1-P hydrogel was printed in solution form, with red (25 G) and blue (22 G) nozzles and addition of PBS.

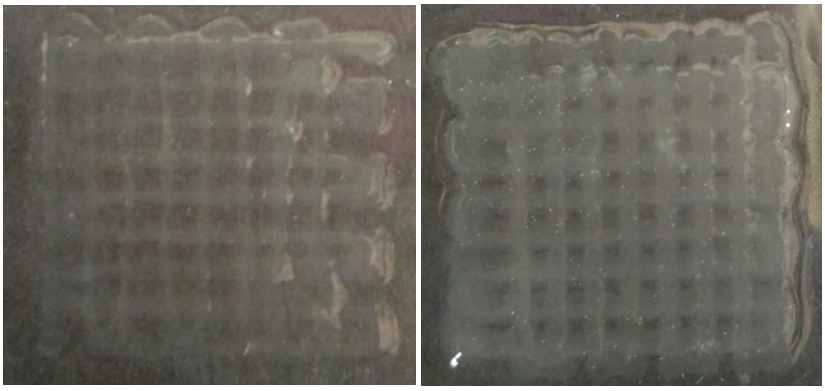

Figure 42. Printed structure of 4 layers in solution form and PBS addition. Left: CS/G1-P with red nozzle. Right: CS/G1-P with blue nozzle.

The CS/β-GP hydrogel was printed in solution form, with blue (22 G) nozzle and addition of PBS.

Figure 43. Printed structure of 4 layers in solution form and PBS addition, CS/β-GP with blue nozzle.

The 3 combinations of parameters showed a well-defined final printed structure, but the best structure was the one printed with CS/β-GP solution that seemed more stable than the structures printed with CS/G1-P solution. This effect of stability is due to CS/β-GP hydrogel is stronger than CS/G1-P hydrogel, as rheological results showed (see paragraph 4.8.), and it can be appreciated in the form of the final printed structure.

As mentioned in paragraph 4.1., the gelation time is shorter for CS/β-GP solution and rheological results showed that the solution is more viscous and stronger (values of G' and G'' are higher) before hydrogel formation, it means, in solution form (see paragraph 4.8.). Both things caused the clogging of the nozzle when a complex structure of 8 layer was tried to be printed. The solution was gelled in the tip of the nozzle as the printing time and the time that the nozzle was in contact with PBS was bigger for a more complex structure of 8 layers, getting unsuccessful results.

On the contrary, a complex structure of 8 layers was achieved with CS/G1-P solution because gelation time is bigger and the solution is less viscous and less strong (values of G' and G'' are lower) in comparison to CS/β-GP solution (see paragraphs 4.1. and 4.6.). The structure was printed with red (25 G) and blue (22 G) nozzles and addition of PBS.

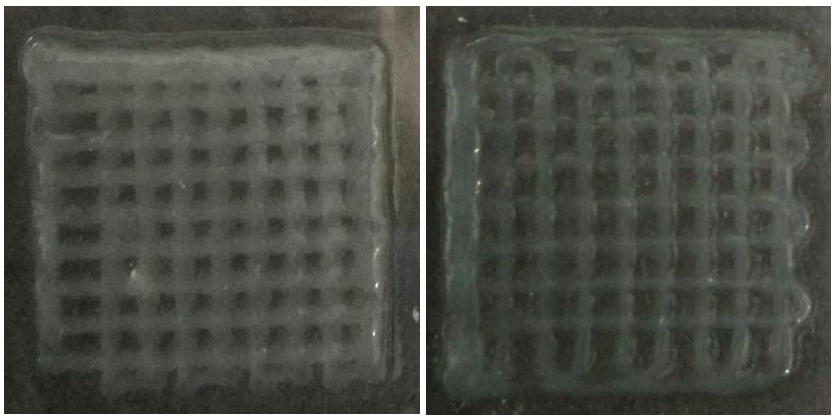

Figure 44. Printed structure of 8 layers in solution form and PBS addition. Left: CS/G1-P with red nozzle. Right: CS/G1-P with blue nozzle.

Results showed that CS/G1-P and CS/β-GP solutions were good ink candidates for bioprinting and the printing conditions affect in a big way the final printed structure, which have to be carefully chosen.

CS/G1-P solution was more manageable as an ink, as it was less viscous and less strong and the gelation time was higher than CS/β-GP solution, while CS/β-GP solution provided more defined structures after printing but causing a lot of problems related with clogging of the nozzle.

The structures were more defined when CS/β-GP solution was used due to the viscosity of the ink. As it is more viscous, the filament maintained its form better once it reached the surface of the Petri dish. The opposite effect was observed when CS/G1-P was used as an ink, which is less viscous and filaments spread once they reached the surface of the Petri dish, for that reason filaments were thicker in comparison to those achieved with CS/β-GP solution.

5. Conclusions

In the first part of this study, the objective was to find a thermo-sensitive hydrogel which turned into gel form with an increase of temperature at 37°C in the shortest possible time and preserve a pH in the physiological range. Three hydrogels presented these characteristics and they were selected as the best candidates. These candidates were:

- CS 80/100 dissolved in β-GP at a final concentration of 1.5% w/v, R equal to 8 and DMEM.
    - T_{gel} = 5 minutes
    - pH = 7.42
- CS 95/100 dissolved in β-GP at a final concentration of 2.5% w/v, R equal to 4 and DMEM.
    - T_{gel} = 5 minutes
    - pH = 7.11
- CS 95/100 dissolved in G1-P at a final concentration of 2% w/v, R equal to 4.5 and DMEM.
    - T_{gel} = 10 minutes
    - pH = 7.02

The degradation test suggested that the hydrogel developed with CS 80/100 was no longer a good candidate as it was degraded after one day in contact with PBS solution.

The other two hydrogels presented the capacity of swelling in contact with PBS solution as they incremented its water content in a ~5% during the experiment. They also had a similar behaviour on the weight loss as it was similar for both hydrogels; the main weight loss was produced in the first day of experiment and it remained constant until the end of the study, where they had lost ~60% of their initial weight. This weight loss can be attributed to a liberation of gelling agent into the sample.

The second part of the study was more focused on rheology and printability studies. Rheology tests allowed to understand the flow behaviour of the selected hydrogels in solution and hydrogel form, and they showed that CS/PP hydrogels possessed shear-thinning properties. Shear-thinning properties characterize the materials by a decrease in viscosity in response to increases in shear rate.

Applying this principle to the bioprinter, it was noted that high shear rates that are present at the nozzle allow materials to flow through the nozzle, and upon deposition, the shear rate decreases, causing a sharp increase in viscosity. So, the idea of printing the hydrogel in different solution, semi-hydrogel and hydrogel form came after rheology studies.

The only form that succeeded in printing was solution form, several problems appeared when the hydrogel was tried to be printed in semi-hydrogel and hydrogel form and these options were discarded.

Besides, the size of the nozzle and the addition of PBS solution affected in a big way the final printed structure and differences using CS/G1-P hydrogel and CS/β-GP hydrogel were noted.

The best combination of parameters to print was to print in solution form, with the blue nozzle (22 G) and with addition of PBS solution. This combination was useful for both hydrogels, but CS/G1-P hydrogel also allowed the printing in the same conditions but with the red nozzle (25 G).

CS/G1-P solution is more manageable as an ink. The low viscosity and strength, and its higher gelation time in comparison to CS/β-GP solution does not cause problems related with clogging of the nozzle, that is what happens in many cases when CS/β-GP solution is tried to be printed.

On the contrary, using CS/β-GP solution, the structures are more defined due to the high viscosity of the ink, which preserves the form of the filament once it reaches the surface of the Petri dish. A different behaviour is observed when CS/G1-P is used as an ink, which is less viscous and filaments spread once they reach the surface of the Petri dish, achieving thicker filaments. The thickness of filaments can be solved using the red nozzle (25 G) with CS/G1-P solution.

CS/G1-P solution exhibits a higher stability of several days in refrigerated conditions in comparison to CS/β-GP solution, that it is stable for less than 4 hours.

The objective of this project was found and good results were obtained. This study was useful to obtain a preliminary idea about a bioink.

6. References

[1] R. Langer and J. Vacanti, "Tissue Engineering," *Science 260,* pp. 920-923, 1993.

[2] P. Bajaj, R. Schweller, A. Khademhosseini, J. West and R. Bashir, "3D Biofabrication Strategies for Tissue Engineering and Regenerative Medicine," *Annual Review of Biomedical Engineering,* pp. 247-276, 2014.

[3] A. Jakus, A. Rutz and R. Shah, "Advancing the field of 3D biomaterial printing," *Biomedical Materials,* 2016.

[4] S. Gungor-Ozkerim, I. Inci, Y. S. Zhang, A. Khademhosseini and M. R. Dokmeci, "Bioinks for 3D bioprinting: an overview," *Biomaterials Science,* 2018.

[5] S. Murphy and A. Atala, "3D bioprinting of tissues and organs," *Nature America,* 2014.

[6] S. Ji and M. Guvendiren, "Recent Advances in Bioink Design for 3D Bioprinting of Tissues and Organs," *Frontiers in Bioengineering and Biotechnology,* 2017.

[7] M. F. Akhtar, M. Hanif and N. M. Ranjha, "Methods of synthesis of hydrogels... A review," *Saudi Pharmaceutical Journal,* 2015.

[8] S. Supper, N. Anton, N. Seidel, M. Riemenschnitter, C. Shoch and T. Vandamme, "Rheological Study of Chitosan/Polyol-phosphate Systems: Influence of the Polyol Part on the Thermo-Induced Gelation Mechanism," *Langmuir,* 2014.

[9] S. Supper, N. Anton, N. Seidel, M. Riemenschnitter, C. Curdy and T. Vandamme, "Thermosensitive chitosan/glycerophosphate-based hydrogel and its derivatives in pharmaceutical and biomedical applications," *Expert Opinion,* 2013.

[10] A. Chenite, C. Chapur, D. Wang and e. al., "Novel injectable neutral solutions of chitosan from biodegradable gels in situ," *Biomaterials,* 2000.

[11] S. Supper, N. Anton, J. Boisclair, N. Seidel, M. Riemenschnitter, C. Curdy and T. Vandamme, "Chitosan/glucose 1-phosphate as new stable in situ forming depot system for controlled drug delivery," *European Journal of Pharmaceutics and Biopharmaceutics,* 2014.

[12] R. Fusaro, "SVILUPPO E CARATTERIZZAZIONE DI IDROGELI TERMOSENSIBILI CHITOSANO/ β-GLICEROFOSFATO PER TERAPIE CELLULARI," 2018.

[13] A. Chenite, M. Buschmann, D. Wang, C. Chaput and n. Kandani, "Rheological characterisation of thermogelling chitosan/glycerol-phosphate solutions," *Carbohydrate Polymers,* pp. 39-47, 2001.

[14] T. G. Mezger, Applied Rheology – With Joe Flow on Rheology Road, Anton Paar, 2014.

[15] M. Laun, "Understanding Rheology of Structured Fluids," *TA Instruments,* 1964.

[16] M. Panalytical, "Optimizing Rheology to Increase Dispersion, Colloidal and Emulsion Stability," *AZO Materials,* 2010.

[17] D. Howard, L. Buttery, K. Shakesheff and S. Roberts, "Tissue engineering: strategies, stem cells and scaffolds," *Journal of Anatomy,* vol. 213, pp. 66-72, 2008.

[18] D. Tuğrul Tolga, I. Gülseren and G. Menemşe, "A bioprintable form of chitosan hydrogel for bone tissue engineering," *Biofabrication 9,* 2017.

[19] K. Roehm and S. Madihaly, "Bioprinted chitosa-gelatin thermosensitive hydrogels using an inexpensive 3D printer," *Biofabrication 10,* 2017.

[20] M. Stanton, J. Samitier and S. Sánchez, "Bioprinting of 3D hydrogels," *Lab on a chip,* 2015.

[21] H. Y. Zhou, L. J. Jiang, P. P. Cao, J. B. Li and X. G. Chen, "Glycerophosphate-based chitosan thermosensitive hydrogels and their biomedical applications," *Carbohydrate polymers,* 2014.

[22] Y. He, F. Yang, H. Zhao, Q. Gao and B. F. J. Xia, "Research on the printability of hydrogels in 3D bioprinting," *Scientific Reports,* 2016.

[23] T. Hinton, Q. Jallerat, R. Palchesko, J. H. Park, M. Grodzicki, H.-J. Shue, M. Ramadan, A. Hudson and A. Feinberg, "Three-dimensional printing of complex biological structures by freeform reversible embedding of suspended hydrogels," *Biomedical Engineering,* 2015.

Annex A

A1. Gcode Commands

Calibration commands

- G21: Sets units to millimetres
- G90: Use absolute coordinates
- G91: Incremental positioning
- M82: Set extruder to absolute positioning
- M83: Set extruder to relative positioning
- M84: Disable motors

Movement Commands

- G0: Rapid linear move
- G1: Linear move
- G2: Move clockwise arc
- G3: Move counter-clockwise arc
- G4 PX: Pause for X milliseconds (dwell)
- X: Move in X-direction
- Y: Move in Y-direction
- Z: Move in Z direction
- F: Set speed for movement (usually in mm/min)
- E: Length of filament to consume
- I: X-offset for arcs
- J: Y-offset for arcs
- K: Z-offset for arcs
- R: Radius of circle for arcs, e.g., G02 X+2.00 Y+0.00 R2.00

Special M codes for the INKREDIBLE (+) 3D Bioprinter

- M712: Set offset from 1 to 2
- M713: Set offset from 1 to 3
- M721: Set offset from 2 to 1
- M723: Set offset from 2 to 3
- M731: Set offset from 3 to 1
- M732: Set offset from 3 to 2

- M750: Homes the printheads
- M751: Places Printhead 1 in the active position
- M752: Places Printhead 2 in the active position
- M753: Retracts both printheads, making way for the LED to be used
- M760: Opens the valve for Printhead 1
- M761: Closes the valve for Printhead 1
- M762: Opens the valve for Printhead 2
- M763: Closes the valve for Printhead 2
- M764: Turns on the UV LED
- M765: Turns off the UV LED
- T1: Change extruder

A2. Gcode two layers' grid

```
M760

G21 ; set units to millimetres

G90 ; use absolute coordinates

M83 ; use relative distances for extrusion

G1 Z0.400 F4800.000 ; move to next layer (0)

M761

G1 E-2.00000 F2400.00000 ; retract

G1 X-14.469 Y0.500 F4800.000 ; move to first infill point

M760

G1 E2.00000 F2400.00000 ; unretract

G1 F600

G1 X18.469 Y0.500 E5.27010 ; infill

M761

G1 E-2.00000 F2400.00000 ; retract

G1 X18.469 Y3.681 F4800.000 ; move to first infill point

M760
```

```
G1 E2.00000 F2400.00000 ; unretract
G1 F600
G1 X-14.469 Y3.681 E5.27010 ; infill
M761
G1 E-2.00000 F2400.00000 ; retract
G1 X-14.469 Y6.862 F4800.000 ; move to first infill point
M760
G1 E2.00000 F2400.00000 ; unretract
G1 F600
G1 X18.469 Y6.862 E5.27010 ; infill
M761
G1 E-2.00000 F2400.00000 ; retract
G1 X18.469 Y10.043 F4800.000 ; move to first infill point
M760
G1 E2.00000 F2400.00000 ; unretract
G1 F600
G1 X-14.469 Y10.043 E5.27010 ; infill
M761
G1 E-2.00000 F2400.00000 ; retract
G1 X-14.469 Y13.223 F4800.000 ; move to first infill point
M760
G1 E2.00000 F2400.00000 ; unretract
G1 F600
G1 X18.469 Y13.223 E5.27010 ; infill
M761
G1 E-2.00000 F2400.00000 ; retract
```

```
G1 X17.904 Y15.537 F4800.000 ; move to first infill point
M760
```

A3. Gcode four layers' grid

```
M107 ; disable fan
G21 ; set units to millimeters
G90 ; use absolute coordinates
M83 ; use relative distances for extrusion
G1 Z0.300 F4800.000 ; move to next layer (0)
G1 E-0.10000 F2400.00000 ; retract
G92 E0 ; reset extrusion distance
G1 Z1.300 F4800.000 ; lift Z
G1 Z0.300 F4800.000 ; restore layer Z
G1 E0.10000 F2400.00000 ; unretract
M760
G1 X-9.850 Y-9.850 E1.37400 F600.000 ; perimeter
G1 X-7.550 Y-9.850 E1.39700 ; perimeter
G1 X-7.550 Y9.850 E1.59400 ; perimeter
G1 X-5.250 Y9.850 E1.61700 ; perimeter
G1 X-5.250 Y-9.850 E1.81400 ; perimeter
G1 X-2.950 Y-9.850 E1.83700 ; perimeter
G1 X-2.950 Y9.850 E2.03400 ; perimeter
G1 X-0.650 Y9.850 E2.05700 ; perimeter
```

```
G1 X-0.650 Y-9.850 E2.25400 ; perimeter

G1 X1.650 Y-9.850 E2.27700 ; perimeter

G1 X1.650 Y9.850 E2.47400 ; perimeter

G1 X3.950 Y9.850 E2.49700 ; perimeter

G1 X3.950 Y-9.850 E2.69400 ; perimeter

G1 X6.250 Y-9.850 E2.71700 ; perimeter

G1 X6.250 Y9.850 E2.91400 ; perimeter

G1 X8.550 Y9.850 E2.93700 ; perimeter

G1 X8.550 Y-9.850 E3.13400 ; perimeter

G1 Z0.600 F600.000 ; move to next layer (1)

G1 E3.91355 F600.000 ; retract

G92 E0 ; reset extrusion distance

G1 Z1.600 F600.000 ; lift Z

G1 X-9.850 Y-8.550 F600.000 ; move to first perimeter point

G1 Z0.600 F600.000 ; restore layer Z

G1 E0.10000 F600.000 ; unretract

G1 X-9.850 Y-6.250 E0.12300 F600.000 ; perimeter

G1 X9.850 Y-6.250 E0.32000 ; perimeter

G1 X9.850 Y-3.950 E0.34300 ; perimeter

G1 X-9.850 Y-3.950 E0.54000 ; perimeter

G1 X-9.850 Y-1.650 E0.56300 ; perimeter

G1 X9.850 Y-1.650 E0.76000 ; perimeter
```

```
G1 X9.850 Y0.650 E0.78300 ; perimeter

G1 X-9.850 Y0.650 E0.98000 ; perimeter

G1 X-9.850 Y2.950 E1.00300 ; perimeter

G1 X9.850 Y2.950 E1.20000 ; perimeter

G1 X9.850 Y5.250 E1.22300 ; perimeter

G1 X-9.850 Y5.250 E1.42000 ; perimeter

G1 X-9.850 Y7.550 E1.44300 ; perimeter

G1 X9.850 Y7.550 E1.64000 ; perimeter

G1 X9.850 Y9.850 E1.66300 ; perimeter

G1 X-9.850 Y9.850 E1.86000 ; perimeter

G1 Z0.900 F600.000 ; move to next layer (2)

G1 E3.91355 F600.000 ; retract

G92 E0 ; reset extrusion distance

G1 Z1.900 F600.000 ; lift Z

G1 X-9.850 Y-9.850 F600.000 ; move to first perimeter point

G1 Z0.900 F600.000 ; restore layer Z

G1 E0.10000 F600.000 ; unretract

G1 X-9.850 Y-9.850 E0.49400 F600.000 ; perimeter

G1 X-7.550 Y-9.850 E0.51700 ; perimeter

G1 X-7.550 Y9.850 E0.71400 ; perimeter

G1 X-5.250 Y9.850 E0.73700 ; perimeter

G1 X-5.250 Y-9.850 E0.93400 ; perimeter
```

```
G1 X-2.950 Y-9.850 E0.95700 ; perimeter

G1 X-2.950 Y9.850 E1.15400 ; perimeter

G1 X-0.650 Y9.850 E1.17700 ; perimeter

G1 X-0.650 Y-9.850 E1.37400 ; perimeter

G1 X1.650 Y-9.850 E1.39700 ; perimeter

G1 X1.650 Y9.850 E1.59400 ; perimeter

G1 X3.950 Y9.850 E1.61700 ; perimeter

G1 X3.950 Y-9.850 E1.81400 ; perimeter

G1 X6.250 Y-9.850 E1.83700 ; perimeter

G1 X6.250 Y9.850 E2.03400 ; perimeter

G1 X8.550 Y9.850 E2.05700 ; perimeter

G1 X8.550 Y-9.850 E2.25400 ; perimeter

M106 S150.45 ; enable fan

G1 Z1.200 F600.000 ; move to next layer (3)

G1 E3.91355 F600.000 ; retract

G92 E0 ; reset extrusion distance

G1 Z2.200 F600.000 ; lift Z

G1 X-9.850 Y-8.550 F600.000 ; move to first perimeter point

G1 Z1.200 F600.000 ; restore layer Z

G1 E0.10000 F600.000 ; unretract

G1 X-9.850 Y-6.250 E0.12300 F600.000 ; perimeter

G1 X9.850 Y-6.250 E0.32000 ; perimeter
```

```
G1 X9.850 Y-3.950 E0.34300 ; perimeter

G1 X-9.850 Y-3.950 E0.54000 ; perimeter

G1 X-9.850 Y-1.650 E0.56300 ; perimeter

G1 X9.850 Y-1.650 E0.76000 ; perimeter

G1 X9.850 Y0.650 E0.78300 ; perimeter

G1 X-9.850 Y0.650 E0.98000 ; perimeter

G1 X-9.850 Y2.950 E1.00300 ; perimeter

G1 X9.850 Y2.950 E1.20000 ; perimeter

G1 X9.850 Y5.250 E1.22300 ; perimeter

G1 X-9.850 Y5.250 E1.42000 ; perimeter

G1 X-9.850 Y7.550 E1.44300 ; perimeter

G1 X9.850 Y7.550 E1.64000 ; perimeter

G1 X9.850 Y9.850 E1.66300 ; perimeter

G1 X-9.850 Y9.850 E1.86000 ; perimeter

G1 E3.91355 F600.000 ; retract

G92 E0 ; reset extrusion distance

G1 Z2.200 F4800.000 ; lift Z

M107 ; disable fan

M761

G0 Z25

M84 ; disable motors
```

A4. Gcode eight layers' grid

```
M107 ; disable fan

G21 ; set units to millimeters

G90 ; use absolute coordinates

M83 ; use relative distances for extrusion

G1 Z0.300 F4800.000 ; move to next layer (0)

G1 E-0.10000 F2400.00000 ; retract

G92 E0 ; reset extrusion distance

G1 Z1.300 F4800.000 ; lift Z

G1 Z0.300 F4800.000 ; restore layer Z

G1 E0.10000 F2400.00000 ; unretract

M760

G1 X-9.850 Y9.850 E1.17700 F600.000 ; perimeter

G1 X-9.850 Y-9.850 E1.37400 ; perimeter

G1 X-7.550 Y-9.850 E1.39700 ; perimeter

G1 X-7.550 Y9.850 E1.59400 ; perimeter

G1 X-5.250 Y9.850 E1.61700 ; perimeter

G1 X-5.250 Y-9.850 E1.81400 ; perimeter

G1 X-2.950 Y-9.850 E1.83700 ; perimeter

G1 X-2.950 Y9.850 E2.03400 ; perimeter

G1 X-0.650 Y9.850 E2.05700 ; perimeter

G1 X-0.650 Y-9.850 E2.25400 ; perimeter
```

```
G1 X1.650 Y-9.850 E2.27700 ; perimeter

G1 X1.650 Y9.850 E2.47400 ; perimeter

G1 X3.950 Y9.850 E2.49700 ; perimeter

G1 X3.950 Y-9.850 E2.69400 ; perimeter

G1 X6.250 Y-9.850 E2.71700 ; perimeter

G1 X6.250 Y9.850 E2.91400 ; perimeter

G1 X8.550 Y9.850 E2.93700 ; perimeter

G1 X8.550 Y-9.850 E3.13400 ; perimeter

G1 X-0.950 Y-9.850 F600.000 ; move inwards before travel

G1 Z0.600 F600.000 ; move to next layer (1)

G1 E3.91355 F600.000 ; retract

G92 E0 ; reset extrusion distance

G1 Z1.600 F600.000 ; lift Z

G1 X-9.850 Y-8.550 F600.000 ; move to first perimeter point

G1 Z0.600 F600.000 ; restore layer Z

G1 E0.10000 F600.000 ; unretract

G1 X-9.850 Y-6.250 E0.12300 F600.000 ; perimeter

G1 X9.850 Y-6.250 E0.32000 ; perimeter

G1 X9.850 Y-3.950 E0.34300 ; perimeter

G1 X-9.850 Y-3.950 E0.54000 ; perimeter

G1 X-9.850 Y-1.650 E0.56300 ; perimeter

G1 X9.850 Y-1.650 E0.76000 ; perimeter
```

```
G1 X9.850 Y0.650 E0.78300 ; perimeter

G1 X-9.850 Y0.650 E0.98000 ; perimeter

G1 X-9.850 Y2.950 E1.00300 ; perimeter

G1 X9.850 Y2.950 E1.20000 ; perimeter

G1 X9.850 Y5.250 E1.22300 ; perimeter

G1 X-9.850 Y5.250 E1.42000 ; perimeter

G1 X-9.850 Y7.550 E1.44300 ; perimeter

G1 X9.850 Y7.550 E1.64000 ; perimeter

G1 X9.850 Y9.850 E1.66300 ; perimeter

G1 X-9.850 Y9.850 E1.86000 ; perimeter

G1 X-10.150 Y-8.550 F600.000 ; move inwards before travel

G1 Z0.900 F600.000 ; move to next layer (2)

G1 E3.91355 F600.000 ; retract

G92 E0 ; reset extrusion distance

G1 Z1.900 F600.000 ; lift Z

G1 X-9.850 Y-9.850 F600.000 ; move to first perimeter point

G1 Z0.900 F600.000 ; restore layer Z

G1 E0.10000 F600.000 ; unretract

G1 X-9.850 Y9.850 E0.29700 F600.000 ; perimeter

G1 X-9.850 Y-9.850 E0.49400 ; perimeter

G1 X-7.550 Y-9.850 E0.51700 ; perimeter

G1 X-7.550 Y9.850 E0.71400 ; perimeter
```

```
G1 X-5.250 Y9.850 E0.73700 ; perimeter

G1 X-5.250 Y-9.850 E0.93400 ; perimeter

G1 X-2.950 Y-9.850 E0.95700 ; perimeter

G1 X-2.950 Y9.850 E1.15400 ; perimeter

G1 X-0.650 Y9.850 E1.17700 ; perimeter

G1 X-0.650 Y-9.850 E1.37400 ; perimeter

G1 X1.650 Y-9.850 E1.39700 ; perimeter

G1 X1.650 Y9.850 E1.59400 ; perimeter

G1 X3.950 Y9.850 E1.61700 ; perimeter

G1 X3.950 Y-9.850 E1.81400 ; perimeter

G1 X6.250 Y-9.850 E1.83700 ; perimeter

G1 X6.250 Y9.850 E2.03400 ; perimeter

G1 X8.550 Y9.850 E2.05700 ; perimeter

G1 X8.550 Y-9.850 E2.25400 ; perimeter

G1 X-10.150 Y-9.850 F600.000 ; move inwards before travel

M106 S150.45 ; enable fan

G1 Z1.200 F600.000 ; move to next layer (3)

G1 E3.91355 F600.000 ; retract

G92 E0 ; reset extrusion distance

G1 Z2.200 F600.000 ; lift Z

G1 X-9.850 Y-8.550 F600.000 ; move to first perimeter point

G1 Z1.200 F600.000 ; restore layer Z
```

```
G1 E0.10000 F600.000 ; unretract

G1 X-9.850 Y-6.250 E0.12300 F600.000 ; perimeter

G1 X9.850 Y-6.250 E0.32000 ; perimeter

G1 X9.850 Y-3.950 E0.34300 ; perimeter

G1 X-9.850 Y-3.950 E0.54000 ; perimeter

G1 X-9.850 Y-1.650 E0.56300 ; perimeter

G1 X9.850 Y-1.650 E0.76000 ; perimeter

G1 X9.850 Y0.650 E0.78300 ; perimeter

G1 X-9.850 Y0.650 E0.98000 ; perimeter

G1 X-9.850 Y2.950 E1.00300 ; perimeter

G1 X9.850 Y2.950 E1.20000 ; perimeter

G1 X9.850 Y5.250 E1.22300 ; perimeter

G1 X-9.850 Y5.250 E1.42000 ; perimeter

G1 X-9.850 Y7.550 E1.44300 ; perimeter

G1 X9.850 Y7.550 E1.64000 ; perimeter

G1 X9.850 Y9.850 E1.66300 ; perimeter

G1 X-9.850 Y9.850 E1.86000 ; perimeter

G1 X-10.150 Y-8.550 F600.000 ; move inwards before travel

G1 Z1.500 F600.000 ; move to next layer (4)

G1 E3.91355 F600.000 ; retract

G92 E0 ; reset extrusion distance

G1 Z2.500 F600.000 ; lift Z
```

```
G1 X-9.850 Y-9.850 F600.000 ; move to first perimeter point

G1 Z1.500 F600.000 ; restore layer Z

G1 E0.10000 F600.000 ; unretract

G1 X-9.850 Y9.850 E0.29700 F600.000 ; perimeter

G1 X-9.850 Y-9.850 E0.49400 ; perimeter

G1 X-7.550 Y-9.850 E0.51700 ; perimeter

G1 X-7.550 Y9.850 E0.71400 ; perimeter

G1 X-5.250 Y9.850 E0.73700 ; perimeter

G1 X-5.250 Y-9.850 E0.93400 ; perimeter

G1 X-2.950 Y-9.850 E0.95700 ; perimeter

G1 X-2.950 Y9.850 E1.15400 ; perimeter

G1 X-0.650 Y9.850 E1.17700 ; perimeter

G1 X-0.650 Y-9.850 E1.37400 ; perimeter

G1 X1.650 Y-9.850 E1.39700 ; perimeter

G1 X1.650 Y9.850 E1.59400 ; perimeter

G1 X3.950 Y9.850 E1.61700 ; perimeter

G1 X3.950 Y-9.850 E1.81400 ; perimeter

G1 X6.250 Y-9.850 E1.83700 ; perimeter

G1 X6.250 Y9.850 E2.03400 ; perimeter

G1 X8.550 Y9.850 E2.05700 ; perimeter

G1 X8.550 Y-9.850 E2.25400 ; perimeter

G1 X-10.150 Y-9.850 F600.000 ; move inwards before travel
```

```
G1 Z1.800 F600.000 ; move to next layer (5)

G1 E3.91355 F600.000 ; retract

G92 E0 ; reset extrusion distance

G1 Z2.800 F600.000 ; lift Z

G1 X-9.850 Y-8.550 F600.000 ; move to first perimeter point

G1 Z1.800 F600.000 ; restore layer Z

G1 E0.10000 F600.000 ; unretract

G1 X-9.850 Y-6.250 E0.12300 F600.000 ; perimeter

G1 X9.850 Y-6.250 E0.32000 ; perimeter

G1 X9.850 Y-3.950 E0.34300 ; perimeter

G1 X-9.850 Y-3.950 E0.54000 ; perimeter

G1 X-9.850 Y-1.650 E0.56300 ; perimeter

G1 X9.850 Y-1.650 E0.76000 ; perimeter

G1 X9.850 Y0.650 E0.78300 ; perimeter

G1 X-9.850 Y0.650 E0.98000 ; perimeter

G1 X-9.850 Y2.950 E1.00300 ; perimeter

G1 X9.850 Y2.950 E1.20000 ; perimeter

G1 X9.850 Y5.250 E1.22300 ; perimeter

G1 X-9.850 Y5.250 E1.42000 ; perimeter

G1 X-9.850 Y7.550 E1.44300 ; perimeter

G1 X9.850 Y7.550 E1.64000 ; perimeter

G1 X9.850 Y9.850 E1.66300 ; perimeter
```

```
G1 X-9.850 Y9.850 E1.86000 ; perimeter

G1 X-10.150 Y-8.550 F600.000 ; move inwards before travel

G1 Z2.100 F600.000 ; move to next layer (6)

G1 E3.91355 F600.000 ; retract

G92 E0 ; reset extrusion distance

G1 Z3.100 F600.000 ; lift Z

G1 X-9.850 Y-9.850 F600.000 ; move to first perimeter point

G1 Z2.100 F600.000 ; restore layer Z

G1 E0.10000 F600.000 ; unretract

G1 X-9.850 Y9.850 E0.29700 F600.000 ; perimeter

G1 X-9.850 Y-9.850 E0.49400 ; perimeter

G1 X-7.550 Y-9.850 E0.51700 ; perimeter

G1 X-7.550 Y9.850 E0.71400 ; perimeter

G1 X-5.250 Y9.850 E0.73700 ; perimeter

G1 X-5.250 Y-9.850 E0.93400 ; perimeter

G1 X-2.950 Y-9.850 E0.95700 ; perimeter

G1 X-2.950 Y9.850 E1.15400 ; perimeter

G1 X-0.650 Y9.850 E1.17700 ; perimeter

G1 X-0.650 Y-9.850 E1.37400 ; perimeter

G1 X1.650 Y-9.850 E1.39700 ; perimeter

G1 X1.650 Y9.850 E1.59400 ; perimeter

G1 X3.950 Y9.850 E1.61700 ; perimeter
```

```
G1 X3.950 Y-9.850 E1.81400 ; perimeter

G1 X6.250 Y-9.850 E1.83700 ; perimeter

G1 X6.250 Y9.850 E2.03400 ; perimeter

G1 X8.550 Y9.850 E2.05700 ; perimeter

G1 X8.550 Y-9.850 E2.25400 ; perimeter

G1 X-10.150 Y-9.850 F600.000 ; move inwards before travel

G1 Z2.400 F600.000 ; move to next layer (7)

G1 E3.91355 F600.000 ; retract

G92 E0 ; reset extrusion distance

G1 Z3.400 F600.000 ; lift Z

G1 X-9.850 Y-8.550 F600.000 ; move to first perimeter point

G1 Z2.400 F600.000 ; restore layer Z

G1 E0.10000 F600.000 ; unretract

G1 X-9.850 Y-6.250 E0.12300 F600.000 ; perimeter

G1 X9.850 Y-6.250 E0.32000 ; perimeter

G1 X9.850 Y-3.950 E0.34300 ; perimeter

G1 X-9.850 Y-3.950 E0.54000 ; perimeter

G1 X-9.850 Y-1.650 E0.56300 ; perimeter

G1 X9.850 Y-1.650 E0.76000 ; perimeter

G1 X9.850 Y0.650 E0.78300 ; perimeter

G1 X-9.850 Y0.650 E0.98000 ; perimeter

G1 X-9.850 Y2.950 E1.00300 ; perimeter
```

```
G1 X9.850 Y2.950 E1.20000 ; perimeter

G1 X9.850 Y5.250 E1.22300 ; perimeter

G1 X-9.850 Y5.250 E1.42000 ; perimeter

G1 X-9.850 Y7.550 E1.44300 ; perimeter

G1 X9.850 Y7.550 E1.64000 ; perimeter

G1 X9.850 Y9.850 E1.66300 ; perimeter

G1 X-9.850 Y9.850 E1.86000 ; perimeter

G1 X-10.150 Y-8.550 F600.000 ; move inwards before travel

G1 E3.91355 F600.000 ; retract

G92 E0 ; reset extrusion distance

G1 Z3.400 F4800.000 ; lift Z

M107 ; disable fan

M761

M763

M765

G0 Z25

M84 ; disable motors
```